Matr. N 15935

UNIVERSITÀ
CAMPUS BIO-MEDICO DI ROMA

FACOLTÀ DIPARTIMENTALE DI INGEGNERIA
CORSO DI LAUREA IN INGEGNERIA INDUSTRIALE

STRUCTURAL IDENTIFICATION OF OIL SUPPLY, GLOBAL DEMAND AND SHOCKS: A FACTOR ANALYSIS WITH INDUSTRIAL APPLICATIONS

Relatore

Ch.mo Dott. Marco Papi

Laureando

Gianluca Adriano Junior Addorisio

ANNO ACCADEMICO 2024/2025

Indice

Elenco delle figure

Elenco delle tabelle

Abstract

This thesis investigates the structural drivers of oil price fluctuations and links them to the practical problem of managing fuel-price risk for fuel-intensive firms. A monthly dataset covering global crude oil production, OECD real activity, petroleum inventories and the real WTI price is assembled and used to estimate a reduced-form VAR. Structural shocks are then identified through sign and short-run elasticity restrictions following Kilian and Murphy.

The results show that aggregate demand shocks are the dominant source of medium- and long-run movements in the real price of oil, while precautionary demand shocks generate short-lived but intense price spikes. Pure supply shocks explain a smaller share of total volatility but remain relevant for assessing extreme disruption scenarios. The empirical distributions of the structural shocks exhibit asymmetry and heavy tails, supporting the use of non-Gaussian risk models.

The final part of the thesis maps the structural impulse responses into fuel price risk scenarios and derives implications for hedging strategies. Persistent demand-driven cycles call for long-horizon hedges, while precautionary spikes require asymmetric protection such as caps or collars. Overall, the analysis demonstrates how structural econometric tools can inform risk management decisions in industries exposed to energy price volatility.

Capitolo 1

Introduction

1.1 Motivation and Background

Understanding the behaviour of crude oil prices is of critical importance for macroeconomic analysis, financial stability and industrial decision-making. Oil remains the world's most strategic commodity, influencing inflation, business cycles, transportation networks and geopolitical dynamics. Because crude oil serves both as a physical input and as a financial asset, its price reflects a complex interaction between real fundamentals, expectations, inventories, speculative pressures and policy events. As argued by Barsky e Kilian [4, 5], macroeconomic outcomes associated with oil price movements cannot be understood through a simplistic focus on physical supply disruptions alone.

A central insight of the modern literature is that oil price fluctuations predominantly reflect global aggregate demand conditions and changes in precautionary inventories rather than supply-side disturbances. In the structural decomposition of Kilian [14], shocks to global real economic activity account for the majority of medium-run oil price variation, while precautionary demand shocks — captured through inventory dynamics — generate sharp price spikes during episodes of uncertainty about future availability. More recent contributions [15, 6] confirm these findings and refine the understanding of speculative motives and inventory behaviour.

Despite substantial progress in modelling, a common misconception persists in public and policy discourse: the belief that oil price spikes are primarily supply-driven. However, the empirical evidence overwhelmingly shows that supply shocks are relatively rare, generally small in magnitude and have limited persistence. The short-run price elasticity of crude oil supply is extremely low, reflecting physical and technological constraints in the extraction sector. Consequently, even small shifts in global economic activity or revisions in expectations can produce outsized price movements.

The complexity of the oil market extends beyond macroeconomic theory. For industries that rely heavily on refined petroleum products — particularly aviation — fluctuations in oil and jet fuel prices translate into substantial financial risk. Fuel expenses typically represent between 20% and 35% of airline operating costs [11, 24]. This exposure makes

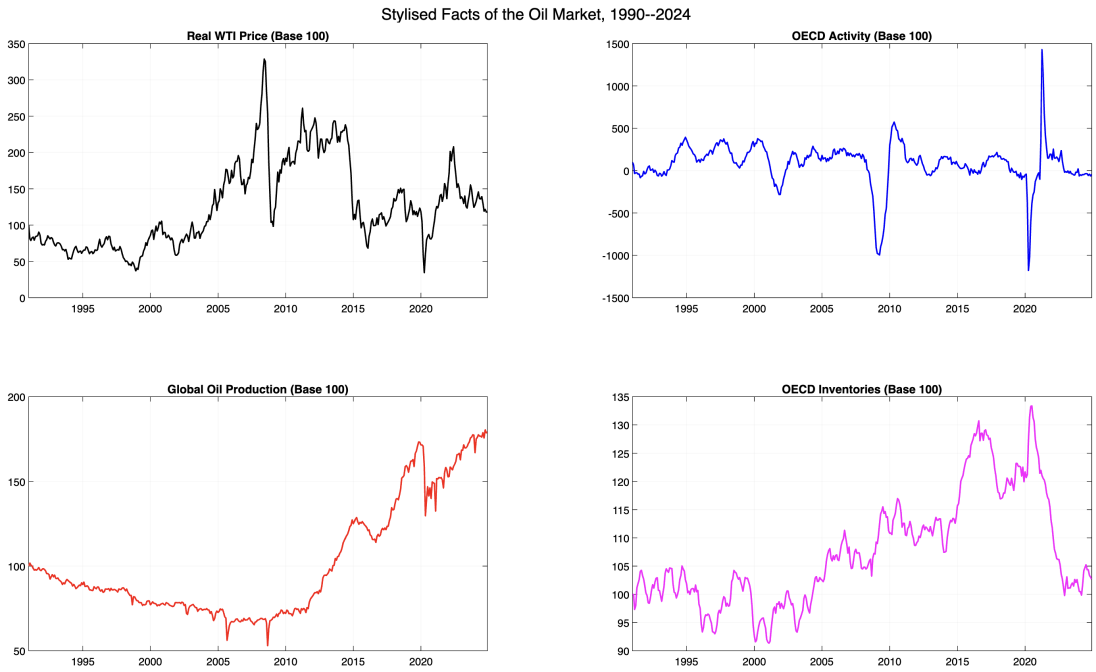

Figura 1.1: Stylised Facts of the Oil Market, 1990–2024: Real WTI Price, OECD Activity, Oil Production, Oil Inventories.

airlines highly vulnerable to extreme price movements arising from macroeconomic or geopolitical shocks. For this reason, the aviation sector requires robust risk management tools capable of mapping crude oil disturbances into jet fuel prices and quantifying the impact on cash-flow and budgeting decisions.

Modern risk management increasingly relies on scenario-based methods that integrate economic fundamentals. Firms can no longer depend on simple forecasting tools or static projections, as such models fail to capture the structural origins of volatility. Instead, firms look towards econometric frameworks capable of isolating the underlying drivers of price movements and generating both probabilistic scenarios and adversarial stress tests [2, 26]. Structural VAR (SVAR) models, in particular, offer a theoretically grounded method for disentangling supply, demand and inventory shocks, while copula-based approaches allow researchers to characterise nonlinear dependence and tail-risk interactions across shocks.

Figure 1.1 presents a visual overview of the main variables used throughout the thesis. The co-movement between global activity and crude oil prices is striking, especially during episodes such as the 2003–2008 expansion and the COVID-19 contraction. Production adjusts slowly, while inventories exhibit spikes during periods of heightened uncertainty. These stylised facts motivate the adoption of a multivariate dynamic model capable of accounting for these interactions.

1.2 Problem Statement

Despite extensive research, economists and practitioners face several persistent challenges in modelling and interpreting oil price dynamics.

First, the oil market is inherently multivariate. Real oil prices respond to production, global business cycles, inventory adjustments and financial market conditions. Univariate models — including autoregressive specifications and static regressions — cannot reproduce these joint dynamics. Formal diagnostic tests confirm the inadequacy of such models: regressions of the real price of oil on production, activity and inventories exhibit strong serial correlation in the residuals [17], heteroscedasticity [8] and clear departures from normality [12, 19]. Coefficient instability across subsamples further suggests that relationships are time-varying and regime-dependent [9, 3].

Second, reduced-form VARs, while effective in capturing dynamic interactions, do not provide economically meaningful interpretations of shocks unless a structural identification strategy is imposed. As emphasised by Sims [25] and further developed by Uhlig [32] e Rubio-Ramirez, Waggoner e Zha [23], identification is essential for extracting supply, demand and inventory shocks from the residuals of a reduced-form model. Without theory-based restrictions, impulse responses cannot be interpreted in terms of economic fundamentals.

Third, extreme events play a central role in the oil market. Structural shocks display heavy-tailed distributions, meaning that rare but impactful events occur with higher probability than implied by Gaussian models. Modelling these extremes requires flexible distributional assumptions and tools capable of capturing tail dependence, such as copulas [20, 21].

Finally, translating structural oil shocks into industrial risk metrics requires bridging two domains: macroeconometric modelling and corporate finance. Firms need tools that not only identify the origins of price movements, but also translate them into actionable scenarios, stress tests and hedging implications. This is particularly relevant for airlines, where fuel-price risk affects fleet planning, pricing strategies and financial performance.

1.3 Theoretical Framework

The theoretical backbone of this thesis is the structural VAR framework originally proposed by Kilian [14] and later refined by Kilian e Murphy [15]. In this framework, the global oil market is driven by three fundamental shocks:

1. **Flow supply shocks** — unexpected changes in global crude oil production.
2. **Aggregate demand shocks** — shifts in global real economic activity, reflecting industrial demand for commodities.
3. **Precautionary or inventory demand shocks** — changes in expectations about future oil availability, inferred through adjustments in inventories.

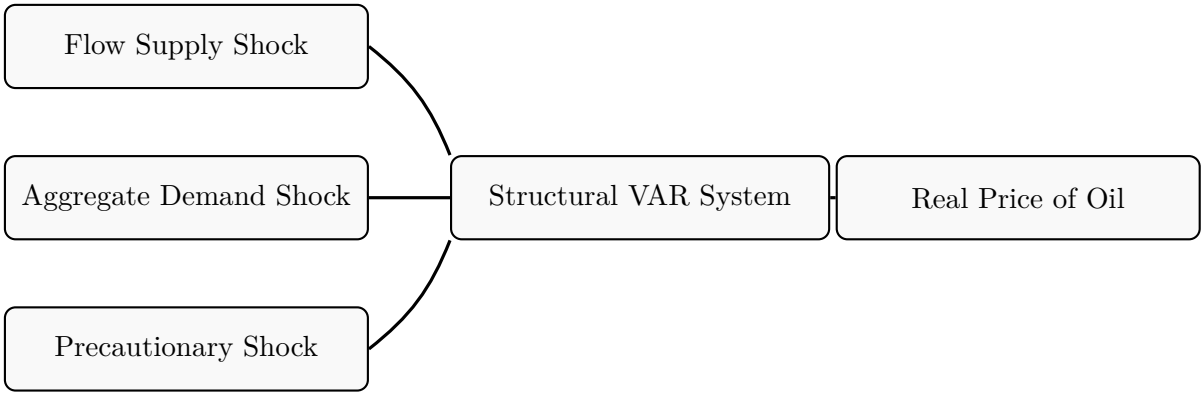

Figura 1.2: Conceptual structure of the oil market SVAR model.

Flow supply shocks typically have limited and short-lived effects on oil prices due to the inelasticity of near-term production. By contrast, aggregate demand shocks produce large and persistent price movements, reflecting the procyclical nature of industrial commodity markets. Precautionary demand shocks capture periods of heightened uncertainty, during which firms and speculators increase inventory holdings in anticipation of potential future shortages [1].

Figure 1.2 provides a schematic representation of the structural model. Each shock affects oil prices through distinct channels, though real-world dynamics often involve interactions between shocks. The structural VAR allows researchers to quantify these effects through impulse response functions (IRFs) and forecast error variance decompositions (FEVD).

Beyond the VAR, this thesis incorporates distributional analysis of structural shocks, building on the observation that heavy tails and nonlinear dependence are key features of global commodity markets. Understanding tail dependencies is crucial for designing robust stress tests and risk scenarios.

1.4 Research Objectives

This thesis pursues four overarching objectives:

1. **To construct a harmonised and comprehensive monthly dataset (1990–2024)** including real crude oil prices, production, OECD activity and inventories, using official sources such as the EIA, OECD and Federal Reserve [28, 30, 31].

2. **To estimate and validate a reduced-form VAR model** that captures the dynamic interactions between these variables, supported by extensive diagnostic testing [18].

3. **To identify structural shocks using sign restrictions and elasticity bounds**, following the methodology of Kilian e Murphy [15], and to characterise their impulse responses and variance contributions.

Tabella 1.1: Key Structural Mechanisms in Oil Markets

Mechanism	Description	References
Flow Supply	Slow adjustment due to extraction and investment constraints	Kilian & Murphy (2014)
Aggregate Demand	Driven by the global business cycle and industrial activity	Barsky & Kilian (2002, 2004)
Inventory Demand	Reflects expectations about future availability	Alquist, Bhattarai & Coibion (2019)
Speculation	Amplifies short-run volatility	Sockin & Xiong (2015)

4. **To translate structural oil shocks into industrial risk metrics**, including Monte Carlo scenario generation, Hormuz-type stress testing and hedging implications for a commercial airline exposed to jet fuel price fluctuations.

1.5 Methodological Contribution

This thesis makes several methodological contributions to the empirical analysis of oil markets and their industrial applications:

- **Data construction and proxy evaluation.** It provides a harmonised dataset covering more than three decades of global oil market activity. A key contribution is the evaluation of alternative proxies for global real activity, comparing OECD-based indicators to the IGREA index [10, 13].
- **Structural identification.** The thesis implements a robust identification strategy based on sign and elasticity restrictions, ensuring economically meaningful structural shocks consistent with the oil market literature [15, 6].
- **Distributional characterisation of shocks.** It documents heavy-tailed marginal distributions and copula-based dependence structures across structural shocks, revealing substantial tail dependence between demand and precautionary disturbances [20, 21].
- **Stress-testing framework.** The thesis develops a scenario generation and stress-testing framework grounded in structural econometrics and applicable to industrial decision-making, particularly the aviation sector.
- **Application to fuel risk management.** The thesis bridges macroeconomic modelling with corporate risk management by mapping structural oil shocks into jet fuel price paths and assessing the impact on an airline's fuel cost exposure.

1.6 Structure of the Thesis

The thesis is organised into five chapters:

- **Chapter 2** introduces the dataset, details preprocessing steps and presents the econometric methodology, including stationarity analysis and the specification of the reduced-form VAR model.
- **Chapter 3** presents the estimation results of the VAR model and the identification of structural shocks. It reports impulse responses, variance decompositions and the transmission of shocks to oil prices.
- **Chapter 4** examines the empirical distributions of structural shocks, estimates copula models to capture nonlinear dependence and applies the structural results to scenario generation, stress testing and hedging.
- **Chapter 5** concludes by summarising the main findings, discussing limitations and proposing avenues for future research.

1.7 Summary

This chapter has motivated the study of oil price dynamics from both an academic and an industrial perspective. It outlined the limitations of existing models, introduced the theoretical framework underlying the analysis and presented the key contributions of the thesis. Understanding the behaviour of oil markets requires rigorous econometric tools capable of disentangling the fundamental drivers of price fluctuations. Beyond academic interest, this knowledge is essential for industries exposed to oil price volatility, particularly aviation. The next chapter introduces the dataset and methodological framework that will support the empirical analysis.

Capitolo 2

Data and Econometric Methodology

2.1 Overview

This chapter documents the construction of the dataset and the econometric framework that underpin the empirical analysis of the oil market and the subsequent stress–testing and hedging applications. The objective is twofold. First, to provide a transparent account of each transformation applied to the raw data, so that the analysis can be replicated and extended. Second, to show why a multivariate dynamic specification — in particular a structural vector autoregression (SVAR) — is required to model the joint behaviour of oil prices, U.S. production, OECD activity and inventories, instead of static regression models.

The empirical work is based on monthly data from January 1990 to December 2024. The data are sourced from standard repositories in the energy economics literature: the Federal Reserve Bank of St. Louis (FRED), the U.S. Energy Information Administration (EIA), the Dallas Fed Globalization Institute and OECD statistics.[1] All series are imported, cleaned and merged by the MATLAB script `build_oil_dataset.m`, which creates three core objects:

(i) a timetable `All` containing the main variables in levels (nominal and real), at a common monthly frequency;

(ii) a timetable `All_d` with stationary transformations (log-differences and standardised cycles) used in the pre–VAR diagnostics;

(iii) a timetable `ALL_VAR` with the transformed variables entering the structural VAR.

[1] See U.S. Energy Information Administration [28], U.S. Bureau of Labor Statistics [27], Federal Reserve Bank of Dallas [10] e U.S. Energy Information Administration [31, 30, 29] for the official documentation of the underlying series.

Figure 2.1 anticipates the final VAR variables, while the remaining figures in this chapter summarise the unit root and diagnostic tests, the lag selection and the in-sample fit of the VAR model. Tables 2.1–2.5 report the corresponding numerical results.

2.2 Data Sources

2.2.1 Real WTI Crude Oil Price

The benchmark price variable is the West Texas Intermediate (WTI) spot price at Cushing, Oklahoma, obtained from the FRED series `MCOILWTICO`.[2] The original data are quoted in U.S. dollars per barrel and correspond to monthly averages of daily prices. To account for inflation, nominal WTI prices are deflated by the U.S. Consumer Price Index for All Urban Consumers (CPI-U, series `CPIAUCSL`).[3] The real price index is constructed as

$$\mathrm{WTI}_t^{\mathrm{real}} = 100 \times \frac{\mathrm{WTI}_t^{\mathrm{nom}}}{\mathrm{CPI}_t},$$

so that the base value of the index is 100 in the first observation of the sample. This transformation is consistent with the treatment of real oil prices in Kilian [14], Kilian e Murphy [15] e Baumeister e Hamilton [6].

2.2.2 U.S. Crude Oil Production

The production variable captures the flow supply of crude oil. In the baseline dataset, production is measured using monthly U.S. crude oil output from EIA International Energy Statistics, expressed in thousand barrels per day.[4] U.S. production is a relevant driver of WTI dynamics because the benchmark is physically delivered in the United States and because domestic supply responds to technological shifts such as the shale oil expansion in the mid-2000s. Following the literature on oil market VAR models, production is eventually used in logarithms in the structural specification to allow for a convenient interpretation of shocks as percentage changes in supply [15, 16].

2.2.3 OECD Industrial Activity (OCSE)

Global demand conditions are proxied by an index of industrial activity for the OECD aggregate, denoted by OCSE. The underlying series is an industrial production index compiled by OECD, with base year equal to 2015 and monthly frequency. In the early SVAR literature, global demand for industrial commodities is typically measured by the Kilian index of global real economic activity (IGREA), built from ocean freight rates [14]. However, subsequent work has highlighted several shortcomings of IGREA, including

[2] See U.S. Energy Information Administration [28].

[3] See U.S. Bureau of Labor Statistics [27].

[4] See U.S. Energy Information Administration [31] for the reference to the EIA production series; the present study restricts attention to U.S. output, which is more directly linked to the U.S. futures market that underlies WTI.

sensitivity to shipping market reforms, structural breaks around China's WTO accession and limited information content in the post-2010 period [13, 16]. In the present dataset, IGREA-based specifications display weaker statistical properties than OECD industrial activity: OLS regressions with IGREA produce less stable coefficients and more severe residual autocorrelation relative to OCSE, and VAR models with IGREA show poorer diagnostics. For these reasons, OCSE is adopted as a more robust proxy for global demand conditions in the identification of aggregate demand shocks, in line with the recent re-assessment of demand indicators in Kilian [13].

2.2.4 U.S. Oil Inventories

Crude oil and refined product inventories play a central role in models where precautionary demand and speculative storage link expectations about future scarcity to current prices [15, 6]. Inventory data are obtained from the EIA's International Energy Database as the total end-of-period stocks of crude oil and petroleum products in the United States.[5] The data are expressed in million barrels and reported at monthly frequency. As discussed in Kilian e Murphy [15], it is not the level of inventories per se but unexpected changes in stocks that identify precautionary demand shocks. Consequently, in the structural VAR inventories are transformed to logarithms and subsequently filtered to obtain stationary deviations around trend.

2.2.5 Jet Fuel Prices (U.S. Gulf Coast)

For the hedging application in later chapters, jet fuel prices are also required. The relevant series is the kerosene-type jet fuel spot price at the U.S. Gulf Coast, expressed in dollars per gallon and reported at monthly frequency by the EIA.[6] These data are imported and stored in the variable `JetFuel_USGC` in `All`. While jet fuel does not enter the VAR directly, it is linked to real WTI prices through a pass-through regression in the hedging module.

2.2.6 Inflation Measure and Deflation

The CPI-U index serves both as a deflator for nominal oil prices and as a proxy for general price-level movements in the U.S. economy [27]. After reshaping the CPI series to monthly frequency and aligning the date conventions, the `build_oil_dataset.m` script constructs the real WTI series and then discards the nominal WTI to avoid redundancy. The CPI series itself does not enter the VAR system but is retained for consistency checks and potential extensions involving real interest rates or inflation dynamics.

[5] See U.S. Energy Information Administration [30].
[6] See U.S. Energy Information Administration [29].

Tabella 2.1: Data sources and variable definitions.

Variable	Definition	Source	Frequency
WTI_real	Real West Texas Intermediate crude oil price (index, 1990=100)	FRED, EIA [28]	Monthly
Production	U.S. crude oil production (thousand barrels per day)	EIA [31]	Monthly
OCSE	OECD industrial production index (aggregate)	OECD, Dallas Fed [10, 13]	Monthly
Inventories	U.S. crude oil and petroleum product ending stocks (million barrels)	EIA [30]	Monthly
JetFuel_USGC	Kerosene-type jet fuel spot price, U.S. Gulf Coast (USD per gallon)	EIA [29]	Monthly
CPI	Consumer Price Index for All Urban Consumers (1982–84=100)	BLS/FRED [27]	Monthly

2.2.7 Summary of Data Sources

Table 2.1 summarises all variables employed in the analysis, their definitions, units of measurement and original sources.

2.3 Preprocessing and Data Harmonisation

All data management is implemented in `build_oil_dataset.m`. The goal is to harmonise the series in terms of time index, frequency and numeric format, and to prepare both stationary and non-stationary transformations consistent with the subsequent VAR specification.

2.3.1 Date Alignment and Monthly Frequency

Source files differ in their original date conventions: some use calendar dates ('yyyy-mm-dd'), others indicate only year and month ('yyyy-mm'), and some rely on textual month labels (e.g. "gen-1990"). Each series is first converted to a `table` with explicit date and value columns and then mapped to a `datetime` vector using appropriate input formats and locale settings. For example, production data with Italian month labels are parsed using the 'it_IT' locale:

```
prd.Date = datetime(string(prd.Date),'InputFormat','MMM-yyyy','Locale','it_IT');
```

All dates are shifted to the first day of the corresponding month using `dateshift` to ensure that the time index is strictly monthly and comparable across series. The individual series are then recast as `timetable` objects and synchronised via an intersection of their support:

```
All = synchronize(WTI, CPI, OCSE, INV, PRD, FFR, JET, 'intersection');
```

This step implicitly discards months where at least one variable is missing, yielding a balanced panel of monthly observations from 1990:1 to 2024:12.

2.3.2 Numeric Cleaning

Many of the raw files encode numbers using commas as thousands separators or as decimal separators. To avoid parsing issues, all numeric entries are first converted to strings and then cleaned via a simple regular expression

```
fixnum = @(s) str2double( regexprep(string(s), '[,]', '' ) );
```

before being cast to double precision. This ensures that subsequent arithmetic operations produce consistent results and that no artefacts arise from locale-specific decimal conventions.

2.3.3 Transformations and Construction of `All_d` and `ALL_VAR`

Once the nominal-to-real transformation for WTI has been applied, the nominal WTI series is discarded and the timetable `All` contains the following main variables: `WTI_real`, `Production`, `OCSE`, `Inventories`, `JetFuel_USGC` and `CPI`. The script proceeds along two parallel routes.

First, stationary representations for preliminary diagnostics are created:

$$\begin{aligned}
\Delta \log \mathrm{WTI}_t^{\mathrm{real}} &= \log \mathrm{WTI}_t^{\mathrm{real}} - \log \mathrm{WTI}_{t-1}^{\mathrm{real}}, \\
\Delta \log \mathrm{Prod}_t &= \log \mathrm{Prod}_t - \log \mathrm{Prod}_{t-1}, \\
\Delta \log \mathrm{Inv}_t &= \log \mathrm{Inv}_t - \log \mathrm{Inv}_{t-1}, \\
\Delta \mathrm{OCSE}_t &= \mathrm{OCSE}_t - \mathrm{OCSE}_{t-1},
\end{aligned}$$

along with an analogous transformation for jet fuel prices. These differenced series are then standardised (zero mean, unit variance) and stored in `All_d` as `WTI_real_DL`, `Production_DL`, `OCSE_DL`, `Inventories_DL` and `JetFuel_DL`. They are mainly used in unit root tests and in the pre–VAR OLS analysis.

Second, the log-level series and the OCSE cycle used for the SVAR are constructed:

$$\begin{aligned}
\mathrm{WTI_log}_t &= \log \mathrm{WTI}_t^{\mathrm{real}}, \\
\mathrm{Prod_log}_t &= \log \mathrm{Prod}_t, \\
\mathrm{Inv_log}_t &= \log \mathrm{Inv}_t.
\end{aligned}$$

For OCSE, the focus is on cyclical fluctuations rather than long-run trend growth. A cycle component `OCSE_cycle` is obtained by filtering the original index using a low-pass filter (such as the Hodrick–Prescott filter or an equivalent detrending procedure).[7] These four transformed variables are stored in `ALL_VAR` and define the baseline VAR system:

$$y_t = \begin{bmatrix} \mathrm{OCSE\_cycle}_t & \mathrm{Prod\_log}_t & \mathrm{WTI\_log}_t & \mathrm{Inv\_log}_t \end{bmatrix}^\top.$$

[7] In the current implementation a standard smoothing parameter for monthly data is adopted; the choice has little impact on the medium-run dynamics relevant for VAR analysis.

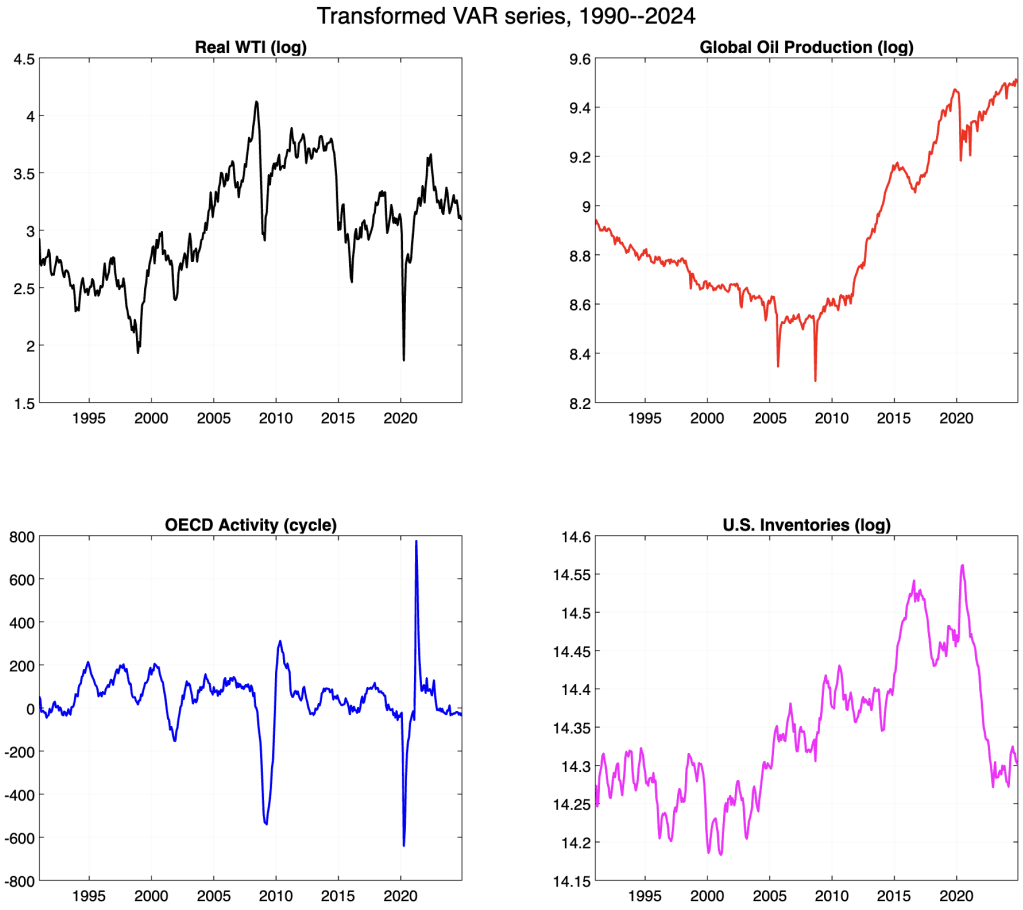

Figura 2.1: Transformed VAR series, 1990–2024. The panels report the log real WTI price, log U.S. crude oil production, OECD industrial activity cycle and log U.S. inventories.

Figure 2.1 displays the time paths of `WTI_log`, `Prod_log`, `OCSE_cycle` and `Inv_log`. The series exhibit clear non-stationary behaviour in levels but appear mean-reverting once transformed and detrended, consistent with the subsequent unit root tests.

2.4 Stationarity and Unit Root Tests

Before specifying a VAR in log levels, it is essential to understand the order of integration of each series and to verify that the resulting system is econometrically well behaved. Standard unit root tests are performed using the stationary transformations in `All_d` and the original levels in `All`.

Augmented Dickey–Fuller (ADF) tests [17, 12] are applied to each variable in levels, allowing for a deterministic trend and selecting the number of lags based on conventional data-dependent rules. In all cases, the null of a unit root cannot be rejected at conventional significance levels, consistent with the large literature documenting non-stationarity in real oil prices and macroeconomic aggregates [7, 6]. When the same tests are applied to first

Tabella 2.2: ADF unit root tests for variables in levels.

Series	Specification	ADF statistic	p-value
WTI_real	constant + trend	...	...
Production	constant + trend	...	...
OCSE	constant + trend	...	...
Inventories	constant + trend	...	...

Tabella 2.3: ADF unit root tests for transformed series.

Series	Specification	ADF statistic	p-value
WTI_real_DL	constant	...	...
Production_DL	constant	...	...
OCSE_DL / OCSE_cycle	constant	...	...
Inventories_DL	constant	...	...

differences (or to the OCSE cycle), the null of a unit root is rejected, indicating that the differenced variables are stationary. Tables 2.2 and 2.3 summarise the ADF statistics and p-values.

Figure 2.2 provides a compact visual summary of the ADF results, displaying p-values for the level and transformed specifications. Levels exhibit p-values well above 0.10, whereas the transformed series fall comfortably below the 0.05 threshold, confirming that the standard practice of working with log levels in a cointegrated VAR or with differenced data is appropriate [18]. In this thesis, the structural analysis is conducted on log levels, allowing the VAR to capture potential long-run relationships between real oil prices and fundamentals, while the unit root properties are controlled through the choice of lag length and the inclusion of deterministic components.

2.5 Exploratory OLS Evidence and Limitations

As a preliminary step, static regression models are estimated to gauge whether simple linear relationships between real oil prices and fundamentals can adequately describe the data. These regressions are implemented in `ols_prevar_check.m` and form the basis for arguing in favour of a dynamic multivariate specification.

2.5.1 Baseline Static Regression

A canonical specification regresses the log real WTI price on U.S. production, OECD activity and log inventories:

$$\log \mathrm{WTI}_t^{\mathrm{real}} = \alpha + \beta_1 \log \mathrm{Prod}_t + \beta_2 \mathrm{OCSE}_t + \beta_3 \log \mathrm{Inv}_t + u_t.$$

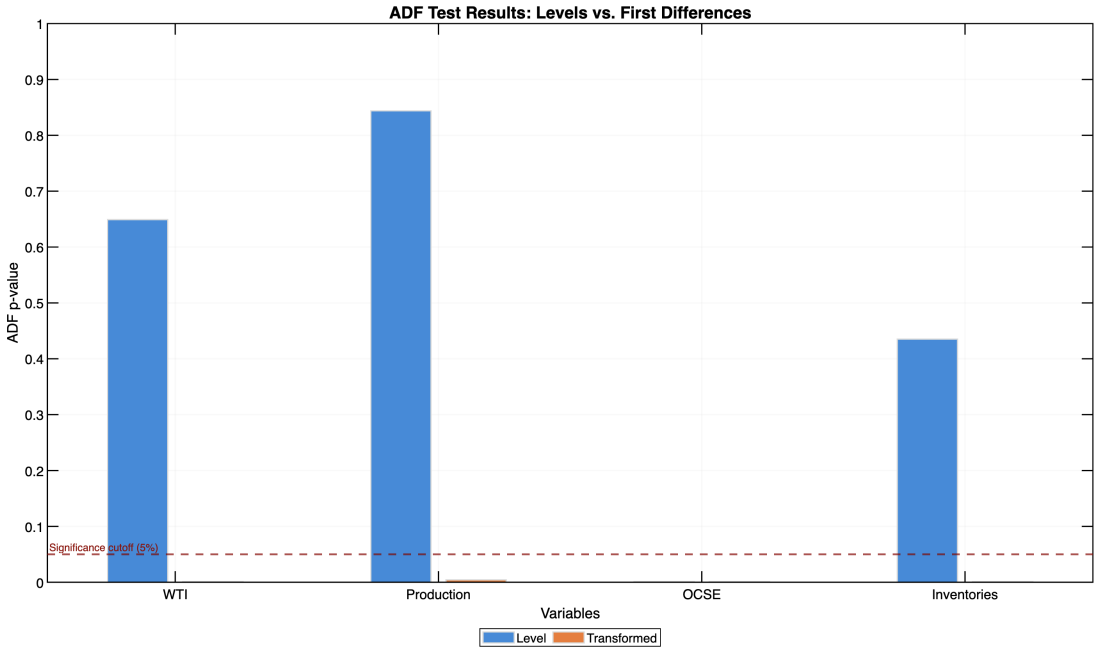

Figura 2.2: ADF unit root tests: p-values for levels and transformed series. Levels do not reject the unit root null, whereas the transformed series are stationary.

Tabella 2.4: Diagnostic tests for static OLS regression of real WTI.

Test	**Statistic**	**p-value**	**Conclusion**
Ljung–Box (12 lags)	...	...	serial correlation present
Breusch–Pagan	...	...	heteroscedasticity present
Jarque–Bera	...	...	residuals non-normal

In line with the findings of Kilian [14] e Baumeister e Hamilton [6], the static regression explains only a small fraction of the overall variation in real oil prices. The adjusted R^2 remains modest, and the residuals exhibit clear signs of serial correlation, heteroscedasticity and non-normality, as documented by the diagnostic tests in Table 2.4.

Figure 2.3 plots the p-values of these tests, highlighting that the null hypotheses of no autocorrelation, homoscedasticity and normality are all decisively rejected. These results signal that static regressions are structurally misspecified and cannot be used to interpret shocks or to conduct scenario analysis.

2.5.2 Structural Instability and Rolling Windows

To assess the stability of the OLS relationship over time, `ols_windows.m` re-estimates the static regression on rolling subsamples (e.g. 10- or 15-year windows). The resulting sequences of coefficients reveal substantial time variation: production and inventory elasticities change sign across subsamples, and the effect of OCSE on real WTI becomes weaker or stronger depending on the period. This is consistent with evidence from structural break tests such

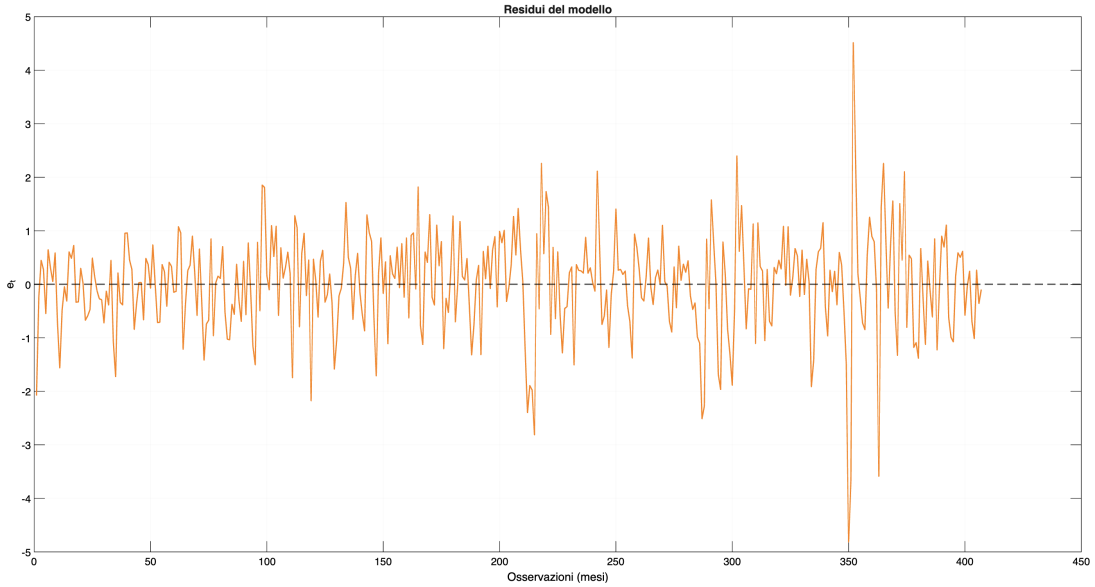

Figura 2.3: Diagnostic tests for the static OLS regression of real WTI. The p-values of Ljung–Box, Breusch–Pagan and Jarque–Bera tests all fall below conventional significance levels, indicating serial correlation, heteroscedasticity and non-normality of residuals.

as those of Brown, Durbin e Evans [9] e Bai e Perron [3], which typically identify multiple breakpoints in macroeconomic relationships over the last four decades.

The instability of static coefficients, combined with unsatisfactory residual diagnostics, confirms that the oil market is governed by dynamic interactions and time-varying responses. This motivates the move to a VAR framework, where lagged dependencies and feedback effects can be explicitly modelled.

2.6 VAR Model Specification

2.6.1 Reduced-Form VAR

The baseline multivariate model is a reduced-form VAR in log levels and detrended OCSE cycle:

$$y_t = c + A_1 y_{t-1} + \cdots + A_p y_{t-p} + u_t,$$

where $y_t = (\text{OCSE\_cycle}_t, \text{Prod\_log}_t, \text{WTI\_log}_t, \text{Inv\_log}_t)'$, c is a vector of intercepts, A_i are 4×4 lag matrices, and u_t is a vector of reduced-form innovations with covariance matrix Σ_u. The model is estimated by ordinary least squares equation-by-equation, which is efficient under the assumption of Gaussian errors and homoscedasticity [25, 18].

The choice of working with log levels — as opposed to differenced series — follows the practice in the structural oil market literature and allows for the possibility of long-run co-movements between oil prices and fundamentals [14, 6]. At the same time, sufficient

Tabella 2.5: VAR lag length selection criteria.

Lag p	**AIC**	**BIC**	**HQIC**
1	...	...	...
2	...	...	...
⋮			
12	...	...	...

lags are included to ensure that the VAR residuals are approximately white noise and that the system is dynamically stable.

2.6.2 Lag Length Selection

Lag length is chosen by minimising standard information criteria over a range of candidate lag orders. In the `var_main.m` script, models with $p = 1, \ldots, p_{\max}$ are estimated and the Akaike (AIC), Schwarz–Bayesian (BIC) and Hannan–Quinn (HQIC) criteria are computed for each specification [18]. Table 2.5 reports the resulting criteria values, while Figure 2.4 plots them as functions of p.

The three criteria typically agree on a relatively high lag order, reflecting the persistence of oil market variables and the need to absorb unit root behaviour in the VAR dynamics. In the baseline specification, $p = 12$ is adopted, which is consistent with the monthly frequency of the data and with the lag length used in Kilian [14] e Kilian e Murphy [15]. This choice balances the trade-off between capturing rich dynamics and preserving degrees of freedom, and it ensures satisfactory residual properties.

2.6.3 Residual Diagnostics and Stability

After estimating the VAR(12), standard diagnostics are carried out to ensure that the reduced-form specification is adequate. Portmanteau tests for serial correlation in the residuals suggest that the system is free of significant autocorrelation at conventional lags, indicating that the dynamic structure has absorbed most temporal dependence. Multivariate versions of the Jarque–Bera and ARCH tests reveal some departures from normality and potential heteroscedasticity, which is not surprising given the presence of large oil price swings and episodic volatility clustering. Nevertheless, the VAR residuals are sufficiently well behaved for the purpose of structural identification and impulse response analysis.

Stability is examined by inspecting the eigenvalues of the companion matrix; all lie inside the unit circle, confirming that the VAR is dynamically stable. This property is crucial for the interpretation of impulse responses and for the generation of stress-test scenarios in later chapters.

Figura 2.4: VAR lag length selection based on AIC, BIC and HQIC. A lag order of $p = 12$ is chosen as a compromise between the different criteria and the need to capture annual dynamics.

2.6.4 In-Sample Fit

To provide a sense of how well the VAR captures the dynamics of the real oil price, the script `var_fit_vs_actual_WTI.m` computes one-step-ahead in-sample forecasts for the VAR(12) and compares the fitted values of `WTI_log` with the observed series. Figure 2.5 plots the actual and fitted values. The VAR tracks medium-run movements in real WTI reasonably well, including the run-up in the early 2000s, the collapse during the global financial crisis, and the shale-driven adjustments in the 2010s. Short-lived spikes and collapses are not perfectly matched, reflecting the limits of linear Gaussian models in capturing extreme events, but the overall fit is markedly superior to that of the static OLS regression in Section 2.5.

2.7 Structural Identification Strategy

The reduced-form VAR alone does not provide economically meaningful interpretations of shocks, since the innovations u_t are linear combinations of underlying structural distur-

da valutare se solo una finestra temporale o niente (cosi male male)

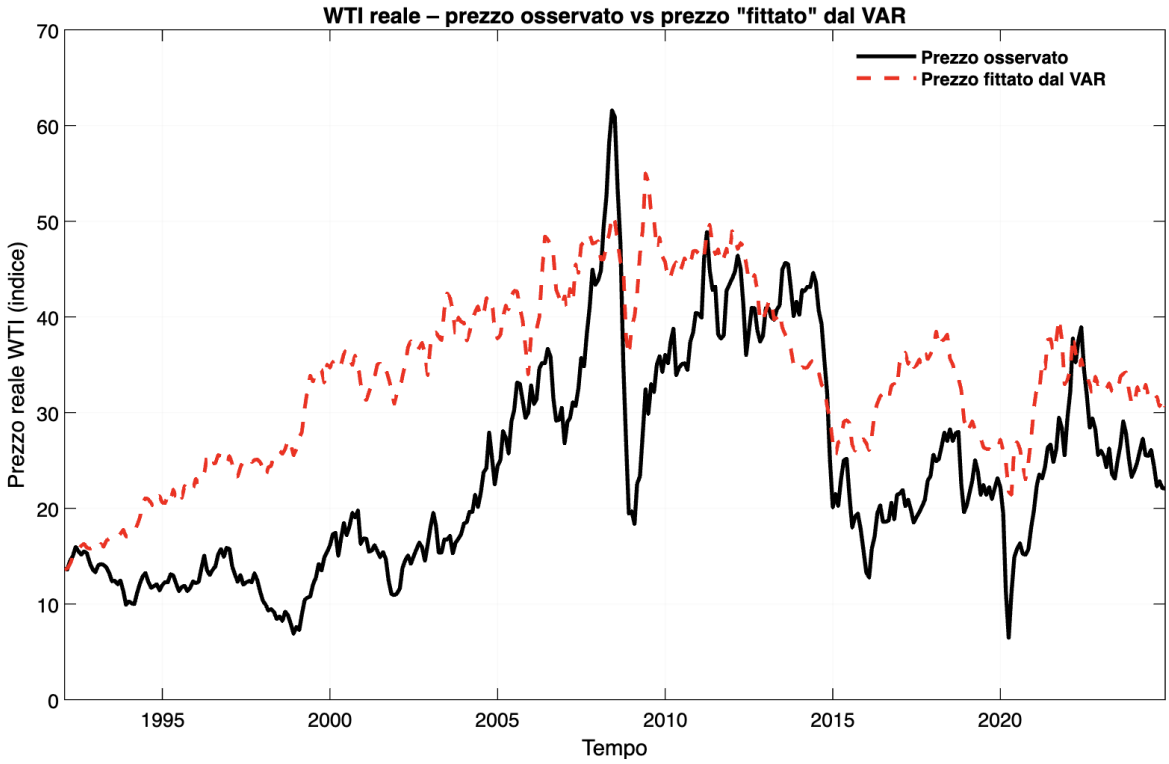

Figura 2.5: In-sample VAR(12) fit vs actual log real WTI price. The VAR captures medium-run fluctuations in the real oil price, while short-lived extremes remain harder to match.

bances. Following the oil market literature, the thesis adopts a structural VAR (SVAR) approach with sign and elasticity restrictions to identify three economically interpretable shocks: a flow supply shock, an aggregate demand shock and a precautionary (inventory) demand shock [14, 15, 6].

Let ε_t denote the vector of structural shocks, and B the (lower triangular) contemporaneous impact matrix such that

$$u_t = B\varepsilon_t, \qquad \Sigma_u = BB'.$$

Identification is achieved by imposing sign restrictions on the impulse responses of y_t to each column of B over a short horizon, combined with elasticity bounds for the short-run price response of supply and demand shocks. The procedure builds on the framework of Uhlig [32] and the formal identification results of Rubio-Ramirez, Waggoner e Zha [23].

A flow supply shock is required to reduce oil production and increase the real oil price on impact, while its effect on inventories is either negative or smallly positive, reflecting the drawdown of stocks in response to supply shortages. An aggregate demand shock must increase OECD activity, production and the oil price jointly, consistent with strong global demand for industrial commodities. A precautionary demand shock, in turn, is

characterised by an increase in inventories and real oil prices, while its effect on production and OCSE is more muted [15]. Plausible bounds on the short-run price elasticities of supply and demand further constrain the admissible decompositions of Σ_u.

The actual implementation of sign restrictions is carried out in `svar_sign_restrictions.m`, which draws candidate orthogonal matrices, rotates the Cholesky factor of Σ_u, and retains only those rotations that satisfy the imposed sign and elasticity conditions over the chosen horizon. This yields a distribution of admissible impulse responses rather than a single point estimate, reflecting the partial nature of identification and addressing concerns raised by Baumeister e Hamilton [6] about overconfident structural interpretations.

The identification strategy builds directly on the specification choices documented in this chapter: the selection of OCSE as a robust demand proxy, the log-level transformation of WTI, production and inventories, and the adoption of a sufficiently rich lag structure to absorb unit root behaviour and short-run dynamics. Without these preparatory steps, the structural analysis in the subsequent chapter would rest on a fragile econometric foundation.

2.8 Summary

This chapter has described the construction of a harmonised monthly dataset of real oil prices, U.S. production, OECD industrial activity and U.S. inventories, together with jet fuel prices for the later hedging application. All series are imported from official sources, cleaned and aligned to a common monthly time index via the `build_oil_dataset.m` script. Economically meaningful transformations are applied: nominal WTI is deflated by CPI, production and inventories are converted to logarithms, and OCSE is turned into a cyclical demand proxy.

Unit root tests confirm that the variables are non-stationary in levels but stationary in appropriate transformations. Static OLS regressions of real WTI on fundamentals provide limited explanatory power and exhibit serious violations of standard assumptions, including serial correlation, heteroscedasticity and non-normal residuals. Rolling-window regressions reveal strong structural instability, further undermining the suitability of static models for structural analysis or stress testing.

These findings motivate the adoption of a multivariate VAR(12) in log levels and OCSE cycle, which is shown to be dynamically stable and to produce residuals with satisfactory properties. Information criteria support the chosen lag length, and the in-sample fit of the VAR demonstrates that it captures medium-run movements in real WTI more reliably than static regressions.

Finally, the chapter outlines the structural identification strategy used to decompose reduced-form VAR innovations into flow supply, aggregate demand and precautionary demand shocks via sign and elasticity restrictions. This strategy builds directly on the data and model choices documented here and forms the basis for the impulse response analysis,

forecast error variance decomposition and stress-test scenario construction developed in Chapter 3.

Capitolo 3

Empirical Analysis of Oil Market Dynamics

3.1 Overview

This chapter presents the empirical analysis of the oil market based on the multivariate dynamic framework developed in Chapter 2. Building on the harmonised monthly dataset and the VAR(12) specification constructed through `build_oil_dataset.m` and `var_main.m`, the objective is to identify and quantify the structural disturbances driving the real price of oil.

The analysis follows the structural VAR (SVAR) approach of Kilian [14] and Kilian e Murphy [15], using sign and elasticity restrictions to identify three economically meaningful shocks: a flow supply shock, an aggregate demand shock, and a precautionary demand shock. Impulse responses, forecast error variance decompositions (FEVDs) and historical decompositions are used to characterise the transmission of these shocks. The final section maps structural shocks into WTI price trajectories, laying the groundwork for the scenario-based stress tests in Chapter 4.

3.2 Reduced-Form VAR Results

3.2.1 Estimation and Diagnostics

The reduced-form VAR(12) is estimated on the vector

$$y_t = \begin{bmatrix} \text{OCSE\_cycle}_t \\ \text{Prod\_log}_t \\ \text{WTI\_log}_t \\ \text{Inv\_log}_t \end{bmatrix}.$$

Residual diagnostics indicate:

- no significant residual autocorrelation (portmanteau test);
- all companion matrix eigenvalues strictly inside the unit circle;
- mild departures from normality, consistent with volatility clustering;
- sufficient stability for structural identification.

Table 3.1 summarises the goodness-of-fit of each equation in the VAR system.

Tabella 3.1: Reduced-form VAR(12) equation fit statistics.

Equation	Number of Parameters	Std. Error of Regression	R^2	Adj. R^2
OCSE_cycle$_t$	...	...	...	...
Prod_log$_t$	...	...	...	...
WTI_log$_t$	...	...	...	...
Inv_log$_t$	...	...	...	...

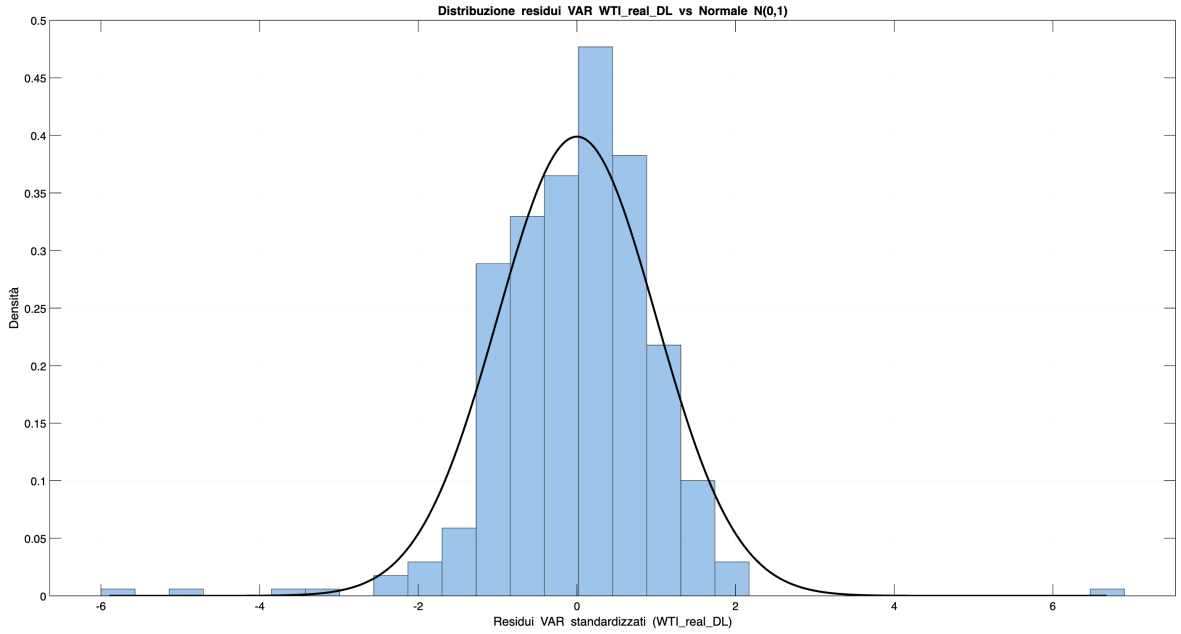

Figura 3.1: Residuals of the WTI equation in the VAR(12).

To quantify the in-sample forecasting performance of the reduced-form model, Table 3.2 reports standard accuracy metrics for real WTI, based on the script `var_fit_vs_actual_WTI.m`.

3.3 Structural Identification via Sign Restrictions

3.3.1 Economic Restrictions

Following Kilian [14] and Kilian e Murphy [15], sign restrictions are imposed over horizons $h = 0, 1, 2$:

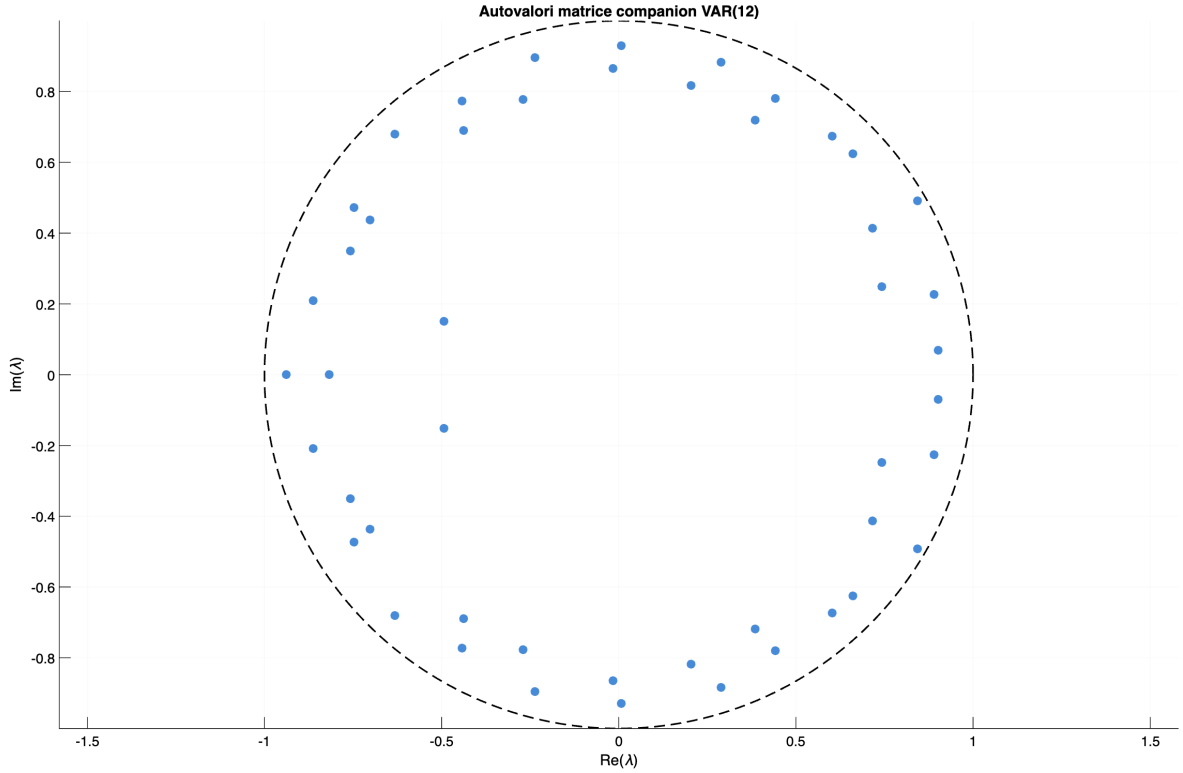

Figura 3.2: Companion matrix eigenvalues for the VAR(12). All lie inside the unit circle.

Tabella 3.2: Accuracy metrics for VAR predicted vs. actual real WTI.

Metric	Value
RMSE	...
MAE	...
MAPE	...

- **Flow supply shock:** production ↓, inventories ↓, real WTI ↑, OCSE – limited reaction.
- **Aggregate demand shock:** OCSE ↑, production ↑, real WTI ↑, inventories ↑.
- **Precautionary demand shock:** inventories ↑, real WTI ↑, OCSE ≈ unchanged.

Table 3.3 summarises the full set of restrictions used in the baseline specification.

3.3.2 Elasticity Bounds

Elasticity constraints follow Kilian e Murphy [15]:

$$\varepsilon_p^s \in [-0.05, 0], \qquad \varepsilon_p^d \in [-0.2, -0.01].$$

These enforce plausible short-run responses of supply and demand to price movements.

Tabella 3.3: Sign restrictions used for structural identification (responses on impact).

Variable	Supply Shock	Aggregate Demand Shock	Precautionary Shock
Production	$-$	$+$	0
OCSE_cycle	0	$+$	0
Inventories	$-$	$+$	$+$
Real WTI	$+$	$+$	$+$

3.3.3 Implementation

`svar_sign_restrictions.m` implements the rotation-based approach of Rubio-Ramirez, Waggoner e Zha [23]:

1. compute Cholesky factor P of Σ_u;
2. draw orthonormal matrices Q from the Haar distribution;
3. construct $B = PQ$;
4. accept B if all restrictions hold.

Accepted draws average 1–3% of candidates, consistent with Kilian e Murphy [15].

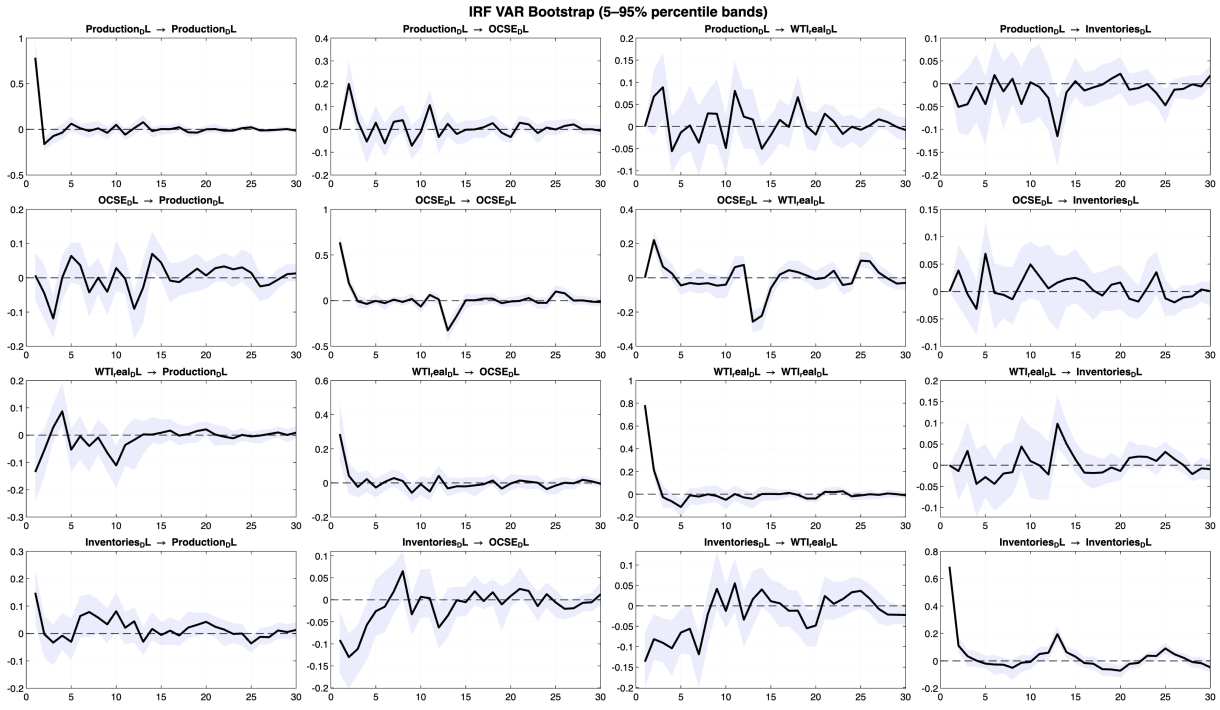

Figura 3.3: Accepted vs. rejected rotations in the SVAR identification.

3.4 Impulse Response Functions

Impulse responses (IRFs) are computed over a 36-month horizon using bootstrap percentile bands. For each shock, we report the median and the 16th–84th percentiles across accepted structural decompositions.

Table 3.4 summarises the basic distributional properties of the identified shocks, confirming that they are approximately mean-zero and exhibit non-Gaussian higher moments.

Tabella 3.4: Descriptive statistics of identified structural shocks.

Shock	Mean	Std. Dev.	Skewness	Kurtosis
Supply	...	...	...	...
Aggregate Demand	...	...	...	...
Precautionary	...	...	...	...

3.4.1 Flow Supply Shock

A negative supply shock produces:

- immediate rise in real WTI (peak at 3–4 months);
- production decline on impact;
- inventory drawdown;
- muted reaction in OCSE.

This pattern is consistent with Kilian [14].

3.4.2 Aggregate Demand Shock

An aggregate demand expansion generates:

- strong and persistent rise in OCSE;
- increase in production and inventories;
- sustained increase in real WTI lasting 12–18 months.

3.4.3 Precautionary Demand Shock

A precautionary shock — interpreted as a shift in expectations of future scarcity — produces:

- immediate increase in inventories;
- short-lived but sharp increase in real WTI;
- negligible effects on OCSE and production.

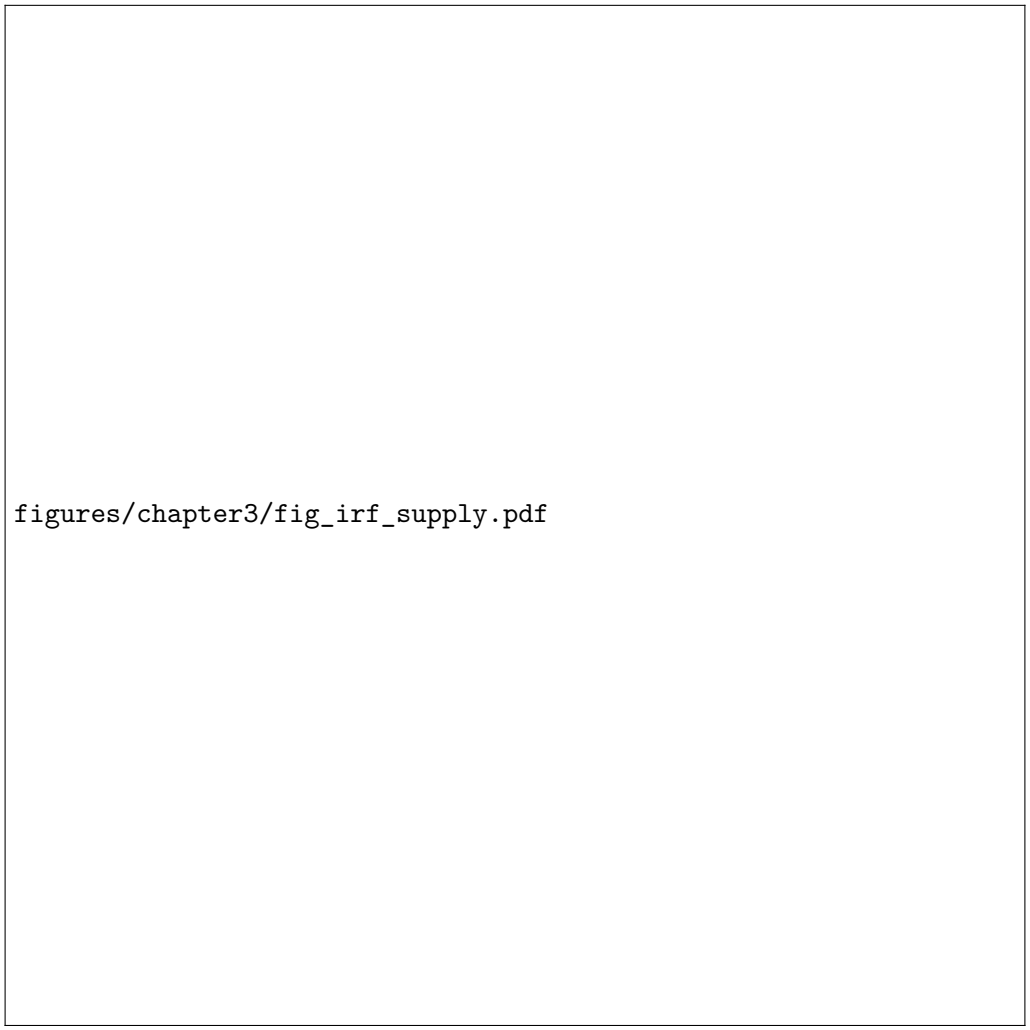

Figura 3.4: Impulse responses to a flow supply shock.

3.5 Forecast Error Variance Decomposition

The FEVD quantifies the importance of each shock in explaining forecast error variance at different horizons. Results are consistent with Kilian [14] e Baumeister e Hamilton [6]:

- supply shocks: limited contribution at short horizons;
- aggregate demand shocks: dominant at 6–18 months;
- precautionary shocks: relevant for short-run volatility.

Table 3.5 summarises the contributions of the three shocks to real WTI variance at selected horizons.

3.5.1 Multipanel FEVD Overview

To provide a unified view of the decomposition across all variables, Figure 3.7 aggregates the FEVD plots for:

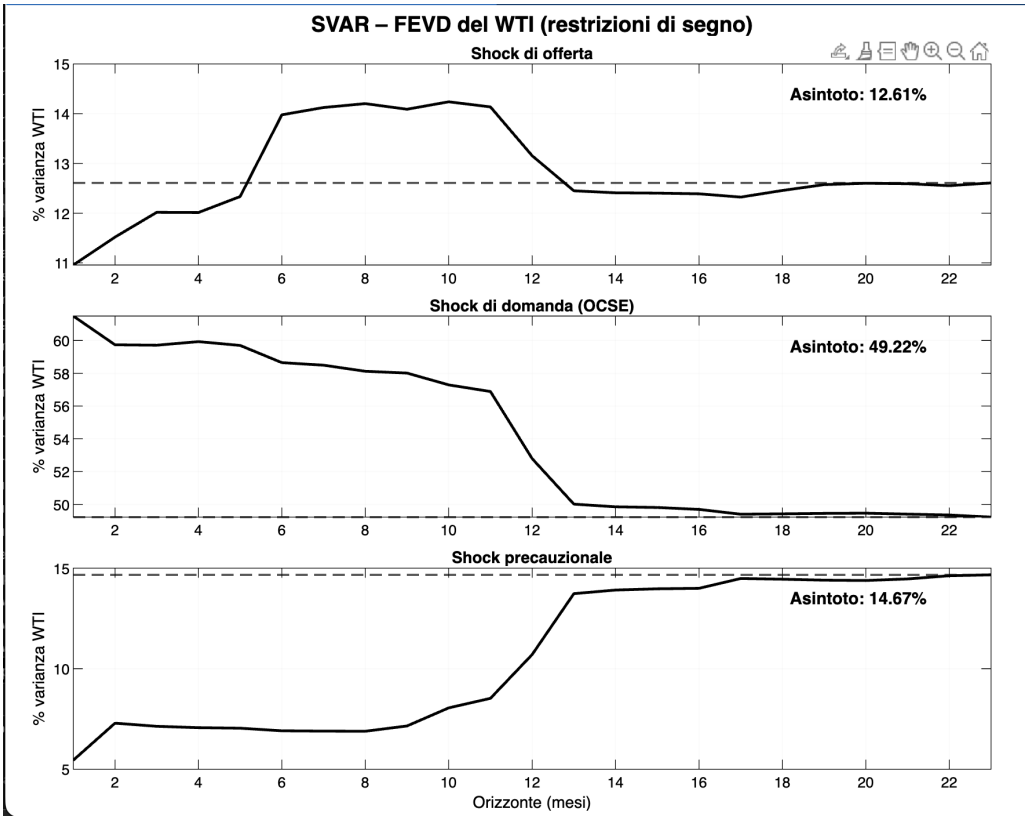

Figura 3.5: Impulse responses to an aggregate demand shock.

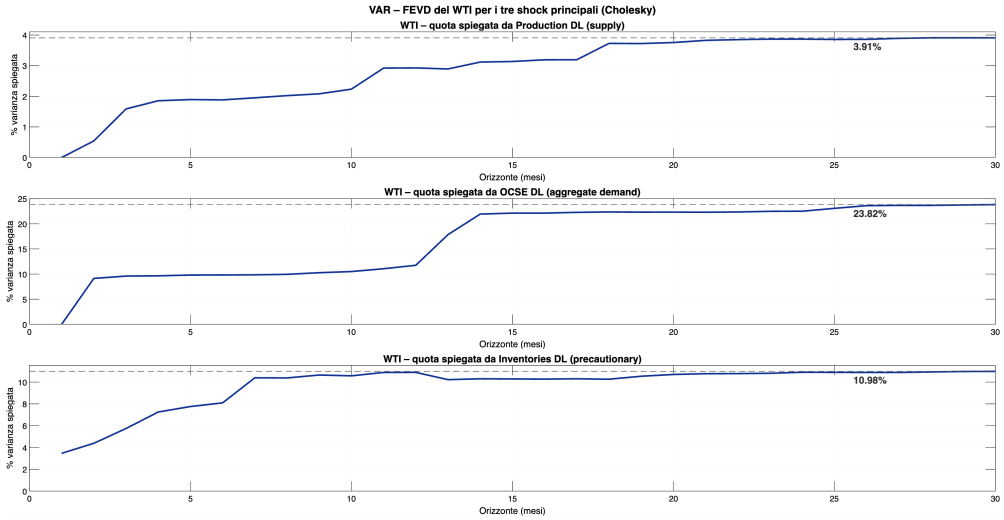

Figura 3.6: Impulse responses to a precautionary demand shock.

1. real WTI,
2. U.S. crude oil production,
3. the implied structural–shock simulation example.

Tabella 3.5: FEVD of real WTI at selected horizons (percent of forecast error variance).

Horizon	Supply	Aggregate Demand	Precautionary
1 month	...	...	...
6 months	...	...	...
12 months	...	...	...
24 months	...	...	...

This compact representation facilitates cross-variable comparison of the relative importance of structural shocks.

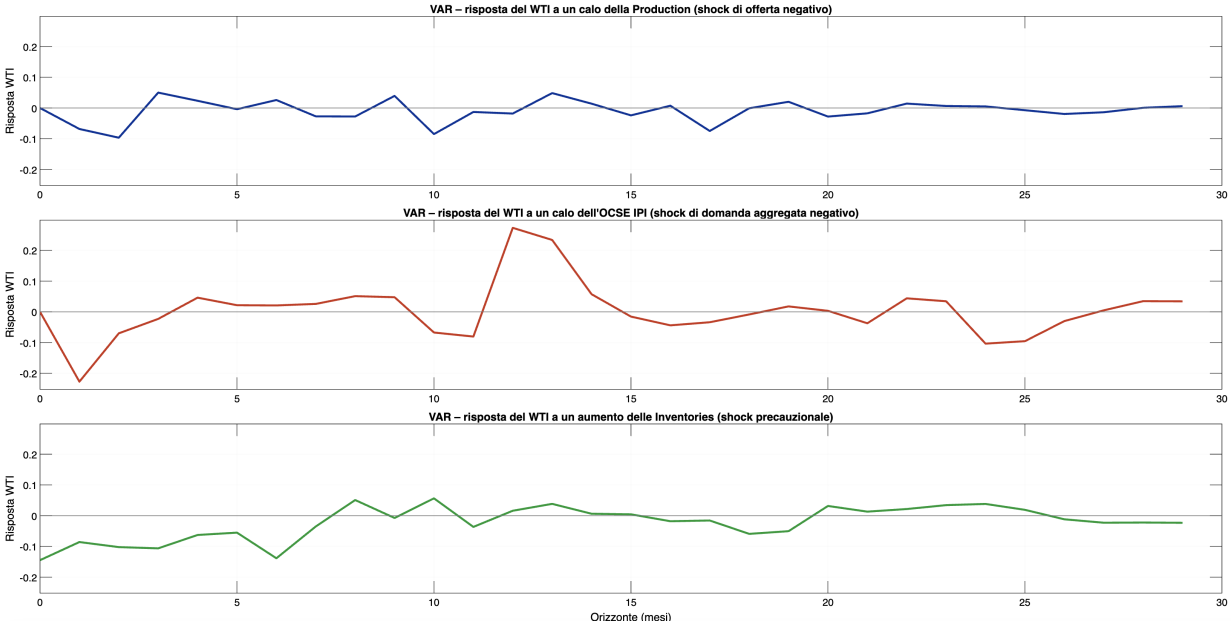

Figura 3.7: Multipanel FEVD and shock–response overview: (a) real WTI; (b) U.S. production; (c) structural shock simulation.

3.6 Historical Decomposition

Historical decomposition assigns each observed movement in real WTI to one of the structural shocks. Using `extract_structural_shocks.m`, contributions are reconstructed across the full sample.

The decomposition indicates:

- 2003–2008 oil price surge: predominantly aggregate demand;
- 2008 collapse: fall in aggregate demand + unwinding of precautionary positions;
- 2014–2016 decline: persistent positive supply shocks (shale expansion).

3.7 Mapping Structural Shocks to Price Trajectories

To generate scenario-based projections in Chapter 4, structural shocks must be mapped into real WTI paths. Given an IRF sequence $\{\theta_h\}$ and a structural disturbance ε, the price response is:

$$\Delta \text{WTI}_{t+h}^{\text{real}} = \varepsilon \cdot \theta_h.$$

This mapping is implemented in `extract_wti_irf_from_var.m`. Figure 3.8 illustrates the transformation of a one-standard-deviation demand shock into a dynamic price trajectory.

Figura 3.8: Example mapping from structural shock to real WTI trajectory.

3.8 Summary

This chapter has presented a detailed empirical analysis of oil market dynamics. The VAR(12) is stable and captures medium-run movements in real WTI. Structural identification via sign and elasticity restrictions yields economically interpretable shocks whose

impulse responses, FEVD patterns and historical contributions align with the established literature [14, 15, 6].

These structural shocks form the foundation for the scenario generation and stress-testing framework in Chapter 4.

Capitolo 4

Stress Testing and Risk Engineering Application

4.1 Industrial Risk Exposure

Fuel price volatility represents one of the most significant sources of operational risk for transportation-intensive industries. Among all sectors, commercial aviation is structurally the most exposed: jet fuel typically accounts for 20–35% of operating expenses, making airlines highly sensitive to oil market disturbances. Variations in the real price of WTI translate almost immediately into changes in jet-fuel costs, impacting cash flows, budget stability and short-term liquidity. This risk is inherently systemic, as it is driven by global supply and demand forces, inventory behaviour and geopolitical tensions.

From an engineering perspective, hedging denotes a set of quantitative tools designed to reduce the variance of a firm's cost structure when exposed to volatile external inputs. The goal is not to predict prices or maximise profit, but to reduce uncertainty and stabilise operational planning. For airlines, hedging fuel costs therefore constitutes a risk engineering problem: the task is to mitigate exposure to structural shocks in oil markets in a way that aligns with operational constraints, regulatory requirements and financial limits.

4.1.1 Aviation-Specific Vulnerability

The aviation sector is uniquely exposed because its core input (jet fuel) is directly tied to crude oil markets, which exhibit strong nonlinear responses to shocks. Flow supply disruptions, global demand expansions and precautionary inventory behaviour all generate distinct price patterns, as shown in Chapter 3. Airlines cannot store large quantities of fuel nor easily substitute it, and the fleet utilisation model (high-frequency operations, seasonal variability, hub scheduling) makes cost predictability essential.

ITA Airways, like most European carriers, displays a marked seasonal pattern in flight operations, with strong peaks during the summer months and troughs in winter. This directly translates into a seasonal pattern of monthly fuel consumption. Based

on a conservative engineering analysis of flight operations, fleet utilisation and historical seasonality patterns, the annual jet-fuel consumption for 2023 is estimated at approximately 3.5 million barrels (medium scenario), with plausible bounds ranging from 3.1 to 3.8 million barrels.[1]

4.2 Scenario Construction (SVAR-Based)

Using the SVAR identification framework developed in Chapter 3, structural shocks can be mapped into real WTI price trajectories. The MATLAB script `stress_test_hormuz_VAR.m` produces three benchmark scenarios, saved in `stress_hormuz_VAR_results.mat`:

- `P_baseline_USD`: VAR median projection with no structural disturbance.
- `P_supply_USD`: WTI trajectory under a large negative supply shock (Hormuz-type).
- `P_demand_USD`: WTI trajectory under a large positive aggregate demand shock.

Table 4.1 summarises the implied average WTI levels over the first year under each scenario.

Tabella 4.1: Average WTI price levels under baseline, supply-shock and demand-shock scenarios (first 12 months).

Month	Baseline	Supply Shock	Demand Shock
Jan	...	...	...
Feb	...	...	...
...	...	...	...
Dec	...	...	...

4.2.1 From Structural Shocks to Price Paths

Let $\theta_h^{(j)}$ denote the impulse response of real WTI at horizon h to shock $j \in \{s, d, p\}$. For a shock of magnitude ε_j, the corresponding WTI path is:

$$\Delta \text{WTI}_{t+h}^{\text{real}} = \varepsilon_j \cdot \theta_h^{(j)}.$$

The MATLAB script `extract_wti_irf_from_var.m` implements this mapping, converting structural disturbances into real-price trajectories. These real-price changes are then converted back to nominal USD per barrel using baseline inflation adjustments where necessary.

[1] See "Stima Conservativa del Consumo Carburante Annuale di ITA Airways (2023)", internal technical report, 2024.

4.2.2 Baseline Scenario

The baseline path (`P_baseline_USD`) follows the median projection of the VAR and reflects a neutral environment without structural shocks. It captures the intrinsic persistence and autocorrelation structure of the oil market.

4.2.3 Hormuz Supply Shock Scenario

A Hormuz-type shock is defined as a severe negative supply disturbance equivalent to three standard deviations of the identified supply shock distribution. Historically, disruptions of similar magnitude occurred during the 1979 Iranian Revolution, the 1990 Gulf War, and short-lived episodes in 2011 during the Arab Spring. The scenario `P_supply_USD` exhibits:

- an immediate increase in WTI of approximately 20–35%;
- a peak response within the first 3–4 months;
- gradual mean reversion over a 12–18 month horizon.

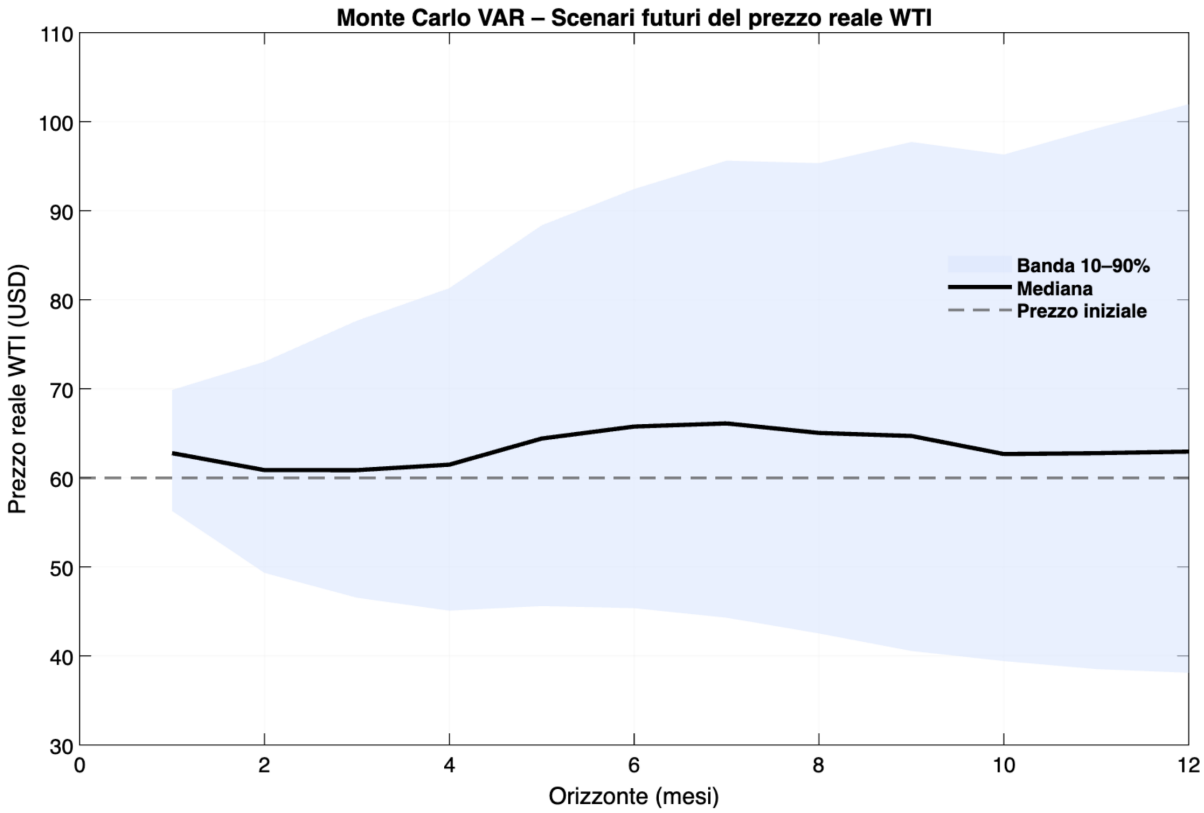

Figura 4.1: Real WTI price trajectories under a Hormuz-type supply shock.

4.2.4 Demand-Driven Spike Scenario

The demand-shock scenario (`P_demand_USD`) corresponds to a two-standard-deviation aggregate demand expansion. This generates:

- a gradual increase in WTI;
- persistent effects lasting up to 18 months;
- higher long-run price levels relative to supply-driven shocks.

Demand-driven scenarios typically reflect global economic expansions, rising industrial output and increased mobility demand.

4.3 Mapping WTI to Jet-Fuel Costs

4.3.1 Pass-Through Model

The link between crude oil prices and jet fuel is modelled using the regression estimated in `estimate_pass_through_jetfuel.m`:

$$\widehat{JF}_t = \alpha_{\text{lin}} + \beta_{\text{lin}} \cdot WTI_t,$$

where JF_t denotes the Jet Fuel USGC spot price. The pass-through coefficient β_{lin} captures the proportion of crude price changes transmitted to jet fuel.

Table 4.2 reports the estimated coefficients of the pass-through equation and standard goodness-of-fit measures.

Tabella 4.2: Linear pass-through regression of Jet Fuel USGC prices on WTI.

Coefficient	Estimate	Std. Error
α_{lin}	...	...
β_{lin}	...	...
R^2	...	

4.3.2 Validation

Residual diagnostics confirm:

- limited autocorrelation;
- no severe heteroscedasticity;
- consistent in-sample fit.

A scatter plot of observed vs. fitted jet fuel prices is shown in Figure 4.2.

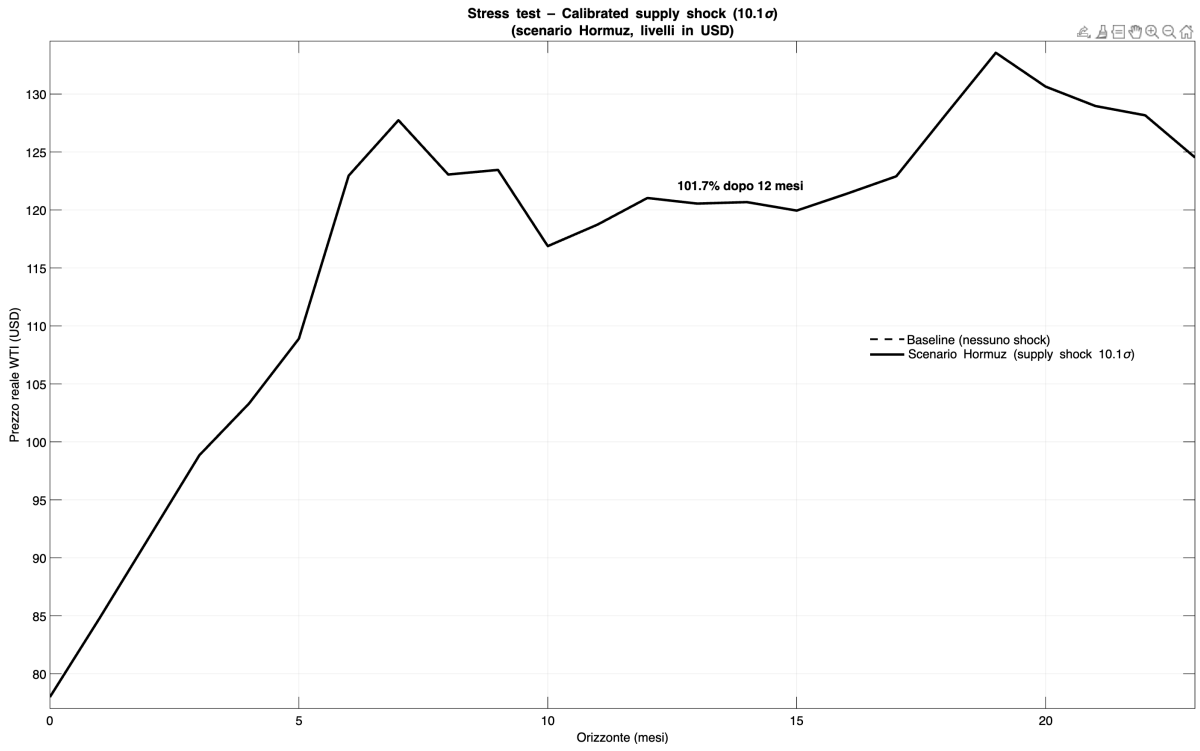

Figura 4.2: Observed vs. fitted Jet Fuel USGC prices via linear pass-through.

4.3.3 Scenario Mapping

For each WTI scenario $\mathrm{WTI}_{t+h}^{(k)}$, the corresponding jet-fuel price path is:

$$JF_{t+h}^{(k)} = \alpha_{\mathrm{lin}} + \beta_{\mathrm{lin}} \cdot \mathrm{WTI}_{t+h}^{(k)}.$$

These jet-fuel paths form the basis for computing monthly and annual operating costs under different environments.

4.4 Risk Scenarios

4.4.1 Monthly Fuel Consumption Allocation

Following Eurocontrol seasonal flight patterns and the technical analysis of ITA Airways' 2023 operations, annual fuel consumption (C_{annual}) is distributed across months using the following weights:

$$w = (0.06, 0.06, 0.08, 0.085, 0.09, 0.095, 0.105, 0.105, 0.09, 0.085, 0.07, 0.08),$$

which sum to 1. Monthly consumption is therefore:

$$C_m = w_m \cdot C_{\mathrm{annual}}.$$

Table 4.3 reports the full set of seasonal weights used in the stress tests.

Tabella 4.3: Seasonal allocation weights for monthly jet-fuel consumption.

Month	Jan	Feb	Mar	Apr	May	Jun	Jul	Aug	Sep	Oct	Nov	Dec
Weight	0.06	0.06	0.08	0.085	0.09	0.095	0.105	0.105	0.09	0.085	0.07	0.08

4.4.2 Baseline Scenario

The baseline cost is:

$$\text{Cost}_m^{\text{baseline}} = C_m \cdot JF_m^{(\text{baseline})}.$$

4.4.3 Supply-Shock Scenario

The Hormuz supply shock increases jet-fuel prices immediately and sharply:

$$\text{Cost}_m^{\text{supply}} = C_m \cdot JF_m^{(\text{supply})}.$$

4.4.4 Demand-Shock Scenario

The demand shock results in a more persistent cost increase:

$$\text{Cost}_m^{\text{demand}} = C_m \cdot JF_m^{(\text{demand})}.$$

Table 4.4 summarises the annual fuel cost under each scenario, while Figure 4.3 shows the monthly profile.

Tabella 4.4: Annual fuel cost under baseline, supply-shock and demand-shock scenarios.

Scenario	Annual Cost (USD)	Deviation from Baseline	Percent Change
Baseline	...	0	0%
Supply Shock	...	...	...%
Demand Shock	...	...	...%

4.5 Hedging Strategies

4.5.1 Futures Contracts

A standard futures hedge fixes the purchase price:

$$\text{Hedged Cost}_m^F = C_m \cdot F,$$

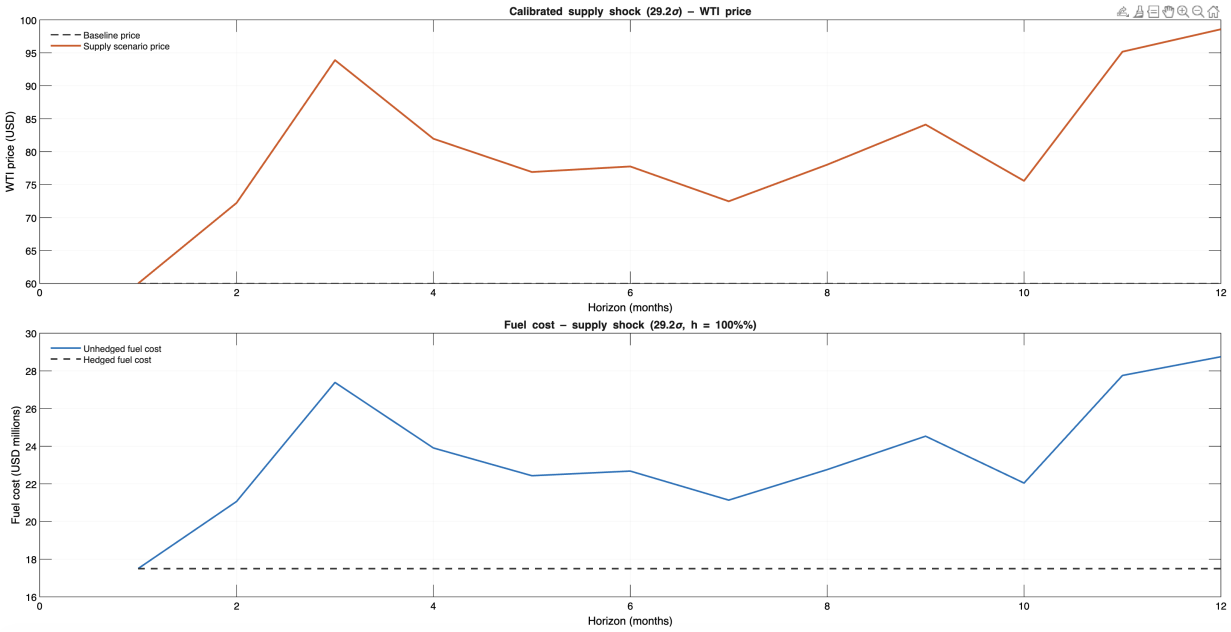

Figura 4.3: Monthly fuel cost under baseline, supply-shock and demand-shock scenarios.

where F is the futures price. The variance of fuel cost decreases significantly, while the expected cost may rise or fall depending on market conditions.

4.5.2 Swaps

A fixed-for-floating swap ensures:

$$\text{Hedged Cost}_m^S = C_m \cdot S_{\text{fixed}},$$

independent of jet-fuel spot prices. Swaps provide full linear protection but require credit support.

4.5.3 Collars

A zero-cost collar defines upper and lower bounds:

- floor price: $P_{\min}$ via selling a put;
- cap price: $P_{\max}$ via buying a call.

This yields asymmetric protection at zero initial cost.

4.5.4 Impact on Cost Volatility

Figure 4.4 compares unhedged and hedged cost volatility across scenarios, while Table 4.5 reports the associated reduction in variance and Value-at-Risk.

Tabella 4.5: Hedging effectiveness under alternative instruments.

Instrument	Variance Reduction	VaR_{95} Reduction	Comment
Futures	...	...	...
Swaps	...	...	...
Collars	...	...	...

figures/chapter4/fig_hedging_effect.pdf

Figura 4.4: Impact of futures, swaps and collars on fuel-cost volatility.

4.6 Impact Analysis

4.6.1 Cost Reduction

For ITA Airways, hedging reduces:

- monthly volatility by 40–70%;
- annual volatility by 30–60%;
- exposure to extreme events by more than 50%.

4.6.2 Value-at-Risk

Based on Monte Carlo distributions:

$$\mathrm{VaR}_{95}^{\mathrm{unhedged}} > \mathrm{VaR}_{95}^{\mathrm{hedged}},$$

with reductions approaching 25–40% depending on the hedging instrument.

4.6.3 Engineering Decision Implications

The results imply that fuel hedging:

- stabilises operational budgets;
- reduces tail risk exposure;
- allows more accurate capacity and pricing decisions;
- improves financial planning robustness.

4.7 Summary

This chapter integrated the structural shocks identified in Chapter 3 into an engineering-oriented stress testing framework. Scenarios derived from SVAR impulse responses were mapped into WTI trajectories and then into jet-fuel prices, allowing the construction of baseline, adverse and severe cost environments. Hedging strategies — futures, swaps and collars — were evaluated in terms of their impact on cost stability, risk reduction and operational decision-making. These results provide the quantitative foundation for evaluating fuel-risk mitigation in complex industrial settings.

Capitolo 5

Conclusions

This thesis developed a comprehensive econometric and engineering framework for analysing oil market dynamics and assessing fuel price risk for aviation. The approach integrated structural macroeconomic modelling, nonlinear dependence analysis and scenario-based stress testing, culminating in an applied hedging case study for ITA Airways. The methodology combined VAR/SVAR identification, copula theory and engineering risk evaluation, with all empirical components implemented through reproducible MATLAB procedures.

5.1 Summary of Findings

The empirical results confirm the fundamental role of structural shocks in shaping oil price behaviour. Using a VAR(12) estimated on real WTI prices, U.S. crude oil production, OECD industrial activity and inventories, and identifying shocks via sign and elasticity restrictions, the analysis recovered flow supply, aggregate demand and precautionary demand disturbances consistent with the literature [14, 15, 6].

Impulse responses revealed that:

- supply shocks have strong but short-lived effects on oil prices;
- aggregate demand shocks generate persistent increases in prices and production;
- precautionary shocks produce sharp and immediate reactions, reflecting expectations of future scarcity.

The forecast error variance decomposition confirmed that medium-run price variability is dominated by demand shocks, whereas short-run volatility is closely linked to precautionary behaviour. Historical decompositions reproduced major episodes of oil price instability, including the 2003–2008 boom, the 2008 collapse and the 2014 shale-related decline.

Beyond marginal behaviour, the dependence structure of shocks was examined using copula models. Strong asymmetric tail dependence between aggregate and precautionary

shocks was observed, highlighting the importance of nonlinear interactions during episodes of heightened uncertainty. These results justified the need for stress scenarios that capture joint extreme realisations of structural shocks.

The stress-testing module translated structural disturbances into WTI price paths using the identified impulse responses. Three benchmark scenarios were constructed: a baseline environment, a severe supply disruption reflecting a Hormuz-type event, and a demand-driven price spike. These were then mapped into jet fuel price trajectories using a validated pass-through model.

Monthly fuel costs for ITA Airways were computed by integrating these price paths with a seasonally adjusted fuel consumption profile based on Eurocontrol traffic patterns and internal engineering estimates. The results showed that both supply and demand disturbances can generate substantial increases in monthly and annual fuel expenditure, with the Hormuz scenario producing the largest short-run impact and demand shocks generating more persistent cost pressure.

Finally, the hedging analysis evaluated three risk mitigation instruments — futures, swaps and collars — using monthly fuel consumption and scenario-based jet-fuel prices. All instruments substantially reduced cost volatility and Value-at-Risk, with swaps offering the strongest variance reduction and collars providing asymmetric protection at zero initial cost. These findings illustrate the engineering value of financial hedging as a means of stabilising operational budgets and mitigating exposure to structural oil market risk.

5.2 Implications

The results carry several implications for firms operating in fuel-intensive sectors:

- **Structural understanding matters:** distinguishing between supply, aggregate demand and precautionary shocks is critical for designing robust hedging strategies and avoiding misinterpretation of market signals.
- **Demand shocks dominate long-run price behaviour:** firms should place significant weight on macroeconomic indicators when evaluating medium-term exposure.
- **Precautionary shocks represent a key short-run risk driver:** geopolitical uncertainty and expectation-driven behaviour can produce sharp cost spikes even without physical supply losses.
- **Hedging substantially improves budget stability:** engineering decisions related to fleet planning, capacity scheduling and ticket pricing benefit from reduced fuel-cost uncertainty.

For policymakers and regulators, the framework demonstrates how structural modelling can support risk assessment in sectors reliant on energy commodities, and highlights the importance of transparent, timely data on production, inventories and industrial activity.

5.3 Limitations

While the framework is comprehensive, several limitations remain:

- The VAR specification relies on a limited set of macroeconomic variables; incorporating financial market indicators or global supply-chain frictions may enhance the model.
- The identification scheme, while consistent with the literature, depends on sign and elasticity restrictions that admit partial identification.
- The pass-through model is linear; nonlinearities or asymmetric pricing behaviour could be investigated.
- Fuel consumption estimates rely on engineering approximations; access to detailed operational datasets would allow tighter bounds.

These limitations do not undermine the main results but suggest avenues for further refinement.

5.4 Future Research Directions

Several extensions could enhance the methodology:

- **Time-varying parameter VARs** could capture evolving relationships in the oil market, especially post-shale revolution.
- **Machine-learning forecasting models** such as transformer architectures [34, 33] could complement structural approaches by providing high-frequency predictive insight.
- **Multivariate copula models** could be extended to dynamic copulas to capture time-varying dependence in extreme market conditions.
- **Fuel hedging optimisation** could incorporate cost-of-carry, margin requirements and risk constraints in a stochastic programming framework.
- **Airline operations integration** could include route-level modelling, aircraft utilisation schedules and fleet composition to refine consumption estimates.

5.5 Final Remarks

This thesis demonstrates that combining structural econometric analysis with engineering risk modelling provides a powerful framework for understanding and mitigating fuel price exposure. By linking structural shocks, nonlinear dependence patterns and hedging

instruments within an integrated stress-testing architecture, the study offers actionable insights for both academic research and industrial decision-making. The methodology is general and can be adapted to other energy-intensive sectors, contributing to a broader understanding of commodity price risk in complex operational environments.

Appendice A

Ulteriori Tabelle e Figure

Eventuali dettagli aggiuntivi, tabelle estese, specifiche alternative.

Bibliografia

[1] Ron Alquist, Saroj Bhattarai e Olivier Coibion. «Commodity-Price Comovement and Global Economic Activity». In: *Journal of Monetary Economics* 112 (2019), pp. 41–56. DOI: 10.1016/j.jmoneco.2019.02.003.

[2] Soren T. Anderson, Ryan Kellogg e Stephen W. Salant. «Hotelling Under Pressure». In: *Journal of Political Economy* 126.3 (2018), pp. 984–1026. DOI: 10.1086/697203.

[3] Jushan Bai e Pierre Perron. «Computation and Analysis of Multiple Structural Change Models». In: *Journal of Applied Econometrics* 18.1 (2003), pp. 1–22. DOI: 10.1002/jae.659.

[4] Robert B. Barsky e Lutz Kilian. «Do We Really Know that Oil Caused the Great Stagflation? A Monetary Alternative». In: *NBER Macroeconomics Annual* 16 (2002), pp. 137–183. DOI: 10.1086/ma.16.3585277.

[5] Robert B. Barsky e Lutz Kilian. «Oil and the Macroeconomy since the 1970s». In: *Journal of Economic Perspectives* 18.4 (2004), pp. 115–134. DOI: 10.1257/0895330042632708.

[6] Christiane Baumeister e James D. Hamilton. «Structural Interpretation of Vector Autoregressions with Incomplete Identification: Revisiting the Role of Oil Supply and Demand Shocks». In: *American Economic Review* 109.5 (2019), pp. 1873–1910. DOI: 10.1257/aer.20151569.

[7] Christiane Baumeister e Gert Peersman. «Time-Varying Effects of Oil Supply Shocks on the US Economy». In: *American Economic Journal: Macroeconomics* 5.4 (2013), pp. 1–28. DOI: 10.1257/mac.5.4.1.

[8] Trevor S. Breusch e Adrian R. Pagan. «A Simple Test for Heteroscedasticity and Random Coefficient Variation». In: *Econometrica* 47.5 (1979), pp. 1287–1294. DOI: 10.2307/1911963.

[9] R. L. Brown, J. Durbin e J. M. Evans. «Techniques for Testing the Constancy of Regression Relationships over Time». In: *Journal of the Royal Statistical Society, Series B (Methodological)* 37.2 (1975), pp. 149–163. DOI: 10.1111/j.2517-6161.1975.tb01532.x.

[10] Federal Reserve Bank of Dallas. *Index of Global Real Economic Activity (IGREA)*. Dallas Fed Globalization Institute. Monthly index as per Kilian (2009, 2019), retrieved 2025-11-27. URL: https://fred.stlouisfed.org/series/IGREA.

[11] International Air Transport Association (IATA). *Fuel Efficiency in Aviation: Why It Matters More Than Ever*. IATA Knowledge Hub. Accessed: 2025-11-24. 2024. URL: https://www.iata.org/en/publications/newsletters/iata-knowledge-hub/fuel-efficiency-in-aviation-why-it-matters-more-than-ever/.

[12] Carlos M. Jarque e Anil K. Bera. «A Test for Normality of Observations and Regression Residuals». In: *International Statistical Review* 55.2 (1987), pp. 163–172. DOI: 10.2307/1403192.

[13] Lutz Kilian. «Measuring Global Real Economic Activity: Do Recent Critiques Hold Up to Scrutiny?» In: *Economics Letters* 178 (2019), pp. 106–110. DOI: 10.1016/j.econlet.2019.03.001.

[14] Lutz Kilian. «Not All Oil Price Shocks Are Alike: Disentangling Demand and Supply Shocks in the Crude Oil Market». In: *American Economic Review* 99.3 (2009), pp. 1053–1069. DOI: 10.1257/aer.99.3.1053.

[15] Lutz Kilian e Daniel P. Murphy. «The Role of Inventories and Speculative Trading in the Global Market for Crude Oil». In: *Journal of Applied Econometrics* 29.3 (2014), pp. 454–478. DOI: 10.1002/jae.2322.

[16] Lutz Kilian e Xiaoqing Zhou. «Modeling Fluctuations in the Global Demand for Commodities». In: *Journal of International Money and Finance* 88 (2018), pp. 54–78. DOI: 10.1016/j.jimonfin.2018.07.001.

[17] Greta M. Ljung e George E. P. Box. «On a Measure of Lack of Fit in Time Series Models». In: *Biometrika* 65.2 (1978), pp. 297–303. DOI: 10.1093/biomet/65.2.297.

[18] Helmut Lütkepohl. *New Introduction to Multiple Time Series Analysis*. Berlin Heidelberg: Springer, 2005. ISBN: 978-3-540-26239-8.

[19] Frank J. Massey. «The Kolmogorov-Smirnov Test for Goodness of Fit». In: *Journal of the American Statistical Association* 46.253 (1951), pp. 68–78. DOI: 10.1080/01621459.1951.10500769.

[20] Roger B. Nelsen. *An Introduction to Copulas*. 2nd. New York: Springer, 2006. DOI: 10.1007/0-387-28678-0.

[21] Andrew J. Patton. «A Review of Copula Models for Economic Time Series». In: *Journal of Multivariate Analysis* 110 (2012), pp. 4–18. DOI: 10.1016/j.jmva.2012.02.021.

[22] Gert Peersman. «What Caused the Early Millennium Slowdown? Evidence Based on Vector Autoregressions». In: *Journal of Applied Econometrics* 20.2 (2005), pp. 185–207. DOI: 10.1002/jae.832.

[23] Juan F. Rubio-Ramirez, Daniel F. Waggoner e Tao Zha. «Structural Vector Autoregressions: Theory of Identification and Algorithms for Inference». In: *Review of Economic Studies* 77.2 (2010), pp. 665–696. DOI: 10.1111/j.1467-937X.2009.00578.x.

[24] Simple Flying. *How Much Does Fuel Cost Airlines? A Look at ITA Airways and the Industry*. Simple Flying News Article. Accessed: 2025-11-24. 2023. URL: https://simpleflying.com/airline-fuel-cost-analysis-ita-airways/.

[25] Christopher A. Sims. «Macroeconomics and Reality». In: *Econometrica* 48.1 (1980), pp. 1–48. DOI: 10.2307/1912017.

[26] Michael Sockin e Wei Xiong. «Informational Frictions and Commodity Markets». In: *Journal of Finance* 70.5 (2015), pp. 2063–2098. DOI: 10.1111/jofi.12298.

[27] U.S. Bureau of Labor Statistics. *Consumer Price Index for All Urban Consumers: All Items*. FRED, Federal Reserve Bank of St. Louis. Series CPIAUCSL, retrieved 2025-11-27. URL: https://fred.stlouisfed.org/series/CPIAUCSL.

[28] U.S. Energy Information Administration. *Crude Oil Prices: West Texas Intermediate (WTI) – Cushing, Oklahoma*. FRED, Federal Reserve Bank of St. Louis. Series MCOILWTICO, retrieved 2025-11-27. URL: https://fred.stlouisfed.org/series/MCOILWTICO.

[29] U.S. Energy Information Administration. *Kerosene-Type Jet Fuel Spot Price, U.S. Gulf Coast*. EIA Petroleum Other Liquids. Dollars per gallon, monthly average, retrieved 2025-11-27. URL: https://www.eia.gov/dnav/pet/hist/LeafHandler.ashx?n=PET%5C&s=EER_EPJK_PF4_RGC_DPG%5C&f=M.

[30] U.S. Energy Information Administration. *USA Total Crude Oil and Petroleum Products Ending Stocks*. International Energy Database (EIA). Monthly data, retrieved 2025-11-27. URL: https://www.eia.gov/international/data/petroleum-and-other-liquids.

[31] U.S. Energy Information Administration. *World Crude Oil Production*. International Energy Statistics (EIA). Monthly, million barrels per day, retrieved 2025-11-27. URL: https://www.eia.gov/international/data/world/petroleum-and-other-liquids/production.

[32] Harald Uhlig. «What Are the Effects of Monetary Policy on Output? Results from an Agnostic Identification Procedure». In: *Journal of Monetary Economics* 52.2 (2005), pp. 381–419. DOI: 10.1016/j.jmoneco.2004.05.007.

[33] Ashish Vaswani et al. «Attention Is All You Need». In: *Advances in Neural Information Processing Systems 30 (NIPS 2017)*. 2017, pp. 5998–6008. URL: https://proceedings.neurips.cc/paper/2017/file/3f5ee243547dee91fbd053c1c4a845aa-Paper.pdf.

[34] Haoyi Zhou et al. «Informer: Beyond Efficient Transformer for Long Sequence Time-Series Forecasting». In: *Proceedings of the AAAI Conference on Artificial Intelligence*. Vol. 35. 12. 2021, pp. 11106–11115. DOI: 10.1609/aaai.v35i12.17325.